Queen Mary
University of London

Hyaluronan and self-assembling peptides as building blocks to reconstruct the extracellular environment in skin tissue

Ferreira, DS; Marques, AP; Reis, RL; Azevedo, HS

• “The final publication is available at RSC via http://pubs.rsc.org/en/content/articlehtml/2013/bm/c3bm60019j”

For additional information about this publication click this link.
http://qmro.qmul.ac.uk/xmlui/handle/123456789/10819

Information about this research object was correct at the time of download; we occasionally make corrections to records, please therefore check the published record when citing. For more information contact scholarlycommunications@qmul.ac.uk

RSC Publishing Biomaterials Science

Hyaluronan and self-assembling peptides as building blocks to reconstruct the extracellular environment in skin tissue

Journal:	*Biomaterials Science*
Manuscript ID:	BM-ART-01-2013-060019.R2
Article Type:	Paper
Date Submitted by the Author:	19-Apr-2013

Complete List of Authors:	Ferreira, Daniela; 3B's Research Group - University of Minho, ; ICVS/3B's - PT Government Associate Laboratory, Marques, Alexandra; University of Minho- 3Bs Research Group, ; 3B's Research Group - University of Minho, ; ICVS/3B's - PT Government Associate Laboratory, Reis, Rui; 3B's Research Group - University of Minho, ; University Minho, Department of Polymer Engineering; ICVS/3B's - PT Government Associate Laboratory, Azevedo, Helena; University of Minho , 3B's Research Group; 3B's Research Group - University of Minho, ; ICVS/3B's - PT Government Associate Laboratory,

SCHOLARONE™
Manuscripts

3B's Research Group
School of Engineering of University of Minho
AvePark, S. Cláudio do Barco
4806-909 Caldas das Taipas, Guimarães, Portugal

April 19th 2013

Prof. Cheng

Associate Editor of *Biomaterials Science, RSC Publishing*

Dear Prof. Cheng,

Thank you for the opportunity to reconsider our manuscript titled "Hyaluronan and self-assembling peptides as building blocks to reconstruct the extracellular environment in skin tissue", by Ferreira et al. (BM-ART-01-2013-060019.R1) for publication in *Biomaterials Science.*

We have noticed that the referee's comments on our revised version are not related with the comments of the referees addressed in the first submission. Anyway, we have responded to the reviewer 3's questions, given below, and we hope these changes address any remaining concerns with this manuscript.

I'm looking forward for your response.

Yours sincerely,

Helena Azevedo

3B's Research Group – University of Minho, AvePark, Zona Industrial da Gandra, S. Cláudio do Barco, 4806-909 Caldas das Taipas, Guimarães, Portugal
Tel: +351 253 510 907 | Fax: +351 253 510909 | www.3bs.uminho.pt | Email: hazevedo@dep.uminho.pt

3B's Research Group
School of Engineering of University of Minho
AvePark, S. Cláudio do Barco
4806-909 Caldas das Taipas, Guimarães, Portugal

Response to referees' comments and text modifications (text highlighted in yellow – changes made in the first revision; text highlighted in blue– changes made in the second revision)

Referee #3

The authors evaluated the potentials of the hyaluronan and self-assembling peptides containing the RGDS sequence for the cell adhesion. The main purpose of this study is to investigate whether incorporation of the RGDS moiety should augment the cell adhesion. The authors' conclusion is not supported by the results and needs further quantitative data. Several serious concerns should be addressed before acceptance of this manuscript.

We are grateful to the referee's comments which we have answered and addressed in the revised manuscript, as described below.

Hyaluronidase-mediated degradation was not evaluated under the standard experimental settings. Seven to fourteen days-of-enzymatic digestions are not a standard way of enzymatic evaluation. Prolonged incubation at 37 degreeC should inactivate the enzymatic activity of hyaluronidase and the results of Day 1.5-Day-14 are not biochemically reliable. The SEM images provide no quantitative information on degradation of hyaluronan moiety.

We thank the reviewer for this important observation and we believe the referee's concern about the non standard experimental settings used on the enzymatic degradation studies is related with loss of enzyme activity with time. We are aware that enzyme deactivation occurs with time and since we have performed enzymatic degradation studies for 14 days we would get loss of enzyme activity during such a long time at 37 ºC. Therefore, we have changed the enzyme solution every 3 days by fresh one. We have followed similar protocols described in the literature for the enzymatic degradation of HA-based biomaterials (Refs. # 1-4). We have forgotten to describe the replenishment of the enzyme solution by fresh one in the manuscript but we have now added it in the revised version.

SEM images of the membranes, before and after degradation, were included in the manuscript to provide additional information on the membrane structure after degradation, since one of the membrane´s component is being degraded by the enzyme, and not to provide quantitative information on the degradation for hyaluronan. The quantification of N-acetylamino sugars in solution really proves HA degradation by hyaluronidase and provides quantitative data. SEM has been widely used to characterize the structure of different biomaterials after degradation, including HA hydrogels (refs. # 3). Therefore, we believe the information provided by SEM is relevant to examine the effect of HA degradation by HAase on the membrane structure, even being a qualitative examination, and to support the other obtained data on the membrane degradation (Fig. 4).

3B's Research Group
School of Engineering of University of Minho
AvePark, S. Cláudio do Barco
4806-909 Caldas das Taipas, Guimarães, Portugal

In general, the presence of serum has a great influence on the cell activity including adhesion and survival. The authors performed a series of experiments under the serum-free conditions. Deprivation of serum might induce apoptotic cell death in the fibroblasts during the prolonged culture period.

We have performed the cell adhesion experiments in the absence of serum to eliminate the complexity of the competing adsorption process of serum proteins on the membrane surface and then mask the effect of the RGDS signal on the adhesion of human dermal fibroblasts (Refs. # 5-7). We are aware that deprivation of serum might induce apoptotic cell death in the fibroblasts during the prolonged culture period and for that reason we have conducted our cell adhesion experiments only for 24 h.

The positive effects of the RGDS sequence on the cell adhesion were supported only by the results of the measurements of DNA content. No dose-dependent effects were observed. Since the number of fluorescent adhesive cells on the materials was not counted, the fluorescence study does not support the authors' hypothesis.

DNA quantification has been widely used for assessing the number of cells and we have used this assay to determine the amount of cells adhered on the different membranes. The results provided by DNA quantification indicate hDFbs adhered at significantly higher number on the membranes containing 50% RGDS than with lower concentration of RGDS, 1 and 10%, or without RGDS (K3-PA and K3DGSR-PA) for all time points except at 12h of culture. We have performed staining of F-actin (phalloidin) and nuclei (DAPI) to investigate the cytoskeleton organization of the cells on the membranes and not for assessing the number of cells on the membranes to corroborate the DNA results. The presence of nuclei also provides information on the amount of cells on the membranes, confirming a higher number of cells on the membranes containing 50% RGDS.

Although the authors investigated the cytoskeletal structure using phalloidin as a probe, the fluorescent images do not exhibit any tendency. It is difficult to discuss something about cytoskeletal changes based on these results.

The reviewer is correct about not observing any tendency on the cytoskeletal organization of the cells adhered on the different membranes. We believe the absence of strong organized actin fibers is related with the low stiffness of the PA-HA membranes used in this study. It is well known that cells cultured on soft substrates show diffuse adhesion complexes with poor actin cytoskeleton organization and the effect of mechanical properties of the substrates are expected to have a major role on the cytoskeletal organization rather the presence of RGDS signal. We have commented this observation in the revised manuscript.

The authors' interpretation of the result of the flow cytometry using an anti-CD44 antibody is inaccurate. The result indicates that about 99% of the cells investigated express CD44 on the

3B's Research Group
School of Engineering of University of Minho
AvePark, S. Cláudio do Barco
4806-909 Caldas das Taipas, Guimarães, Portugal

cell surface and it remains to be determined whether the surface expression levels of CD44 is higher or not.

We would like to refer that we have performed flow cytometry on human fibroblasts, cells used in this study, following the comment of one of the reviewers on the first submission, who has asked us to comment on the presence of CD44 on fibroblasts and how they could also be contributing to cell adhesion to hyaluronan. To answer to the reviewer's comment, we have performed flow cytometry, which confirmed the presence of CD44 in high percentage on the surface of the cells. However, we have cultured the cells on the peptide side and we believe, therefore, that CD44, although present on the fibroblast surface, is not engaged on the adhesion of the cultured cells on the membranes. We have commented this in the revised manuscript.

The involvement of the RGDS sequence and integrins on the cell adhesion could be verified using the specific antibodies.

We thank the reviewer's suggestion and we believe this examination would be highly relevant in this study since the cells were cultured on the peptide side of the membrane, in contact with RGDS, and therefore integrins are expected to be involved on the adhesion of cells on the membranes. Knowing the importance of this additional result to confirm our hypothesis, we have performed immunostaining of $\alpha_v\beta_5$ to detect if these cell-surface integrins were expressed by the cells cultured on the membranes. However, our membrane interferes with the staining process, not being possible to get clear images. Alternative techniques, such as western blot and RT-PCR, are being tested and optimized to be used in further experiments.

References

1. Burdick JA, Chung C, Jia XQ, Randolph MA, Langer R. Controlled degradation and mechanical behavior of photopolymerized hyaluronic acid networks. *Biomacromolecules* 2005, 6:386-391.
2. Park YD, Tirelli N, Hubbell JA. Photopolymerized hyaluronic acid-based hydrogels and interpenetrating networks. *Biomaterials* 2003, 24:893-900.
3. Luo Y, Kirker KR, Prestwich GD. Cross-linked hyaluronic acid hydrogel films: new biomaterials for drug delivery. *Journal of Controlled Release* 2000, 69:169-184.
4. Dhanasingh A, Salber J, Moeller M, Groll J. Tailored hyaluronic acid hydrogels through hydrophilic prepolymer cross-linkers. *Soft Matter* 2010, 6:618-629.
5. Storrie H, Guler MO, Abu-Amara SN, Volberg T, Rao M, Geiger B, Stupp SI. Supramolecular crafting of cell adhesion. *Biomaterials* 2007, 28:4608-4618.
6. Massia SP, Hubbell JA. An RGD spacing of 440 nm is sufficient for integrin alpha V beta 3-mediated fibroblast spreading and 140 nm for focal contact and stress fiber formation. *The Journal of Cell Biology* 1991, 114:1089-1100.

3B's Research Group
3B's Research Group
School of Engineering of University of Minho
AvePark, S. Cláudio do Barco
4806-909 Caldas das Taipas, Guimarães, Portugal

ICVS/3B's
Associate Laboratory
University of Minho

7. Mi LX, Fischer S, Chung B, Sundelacruz S, Harden JL. Self-assembling protein hydrogels with modular integrin binding domains. *Biomacromolecules* 2006, 7:38-47.

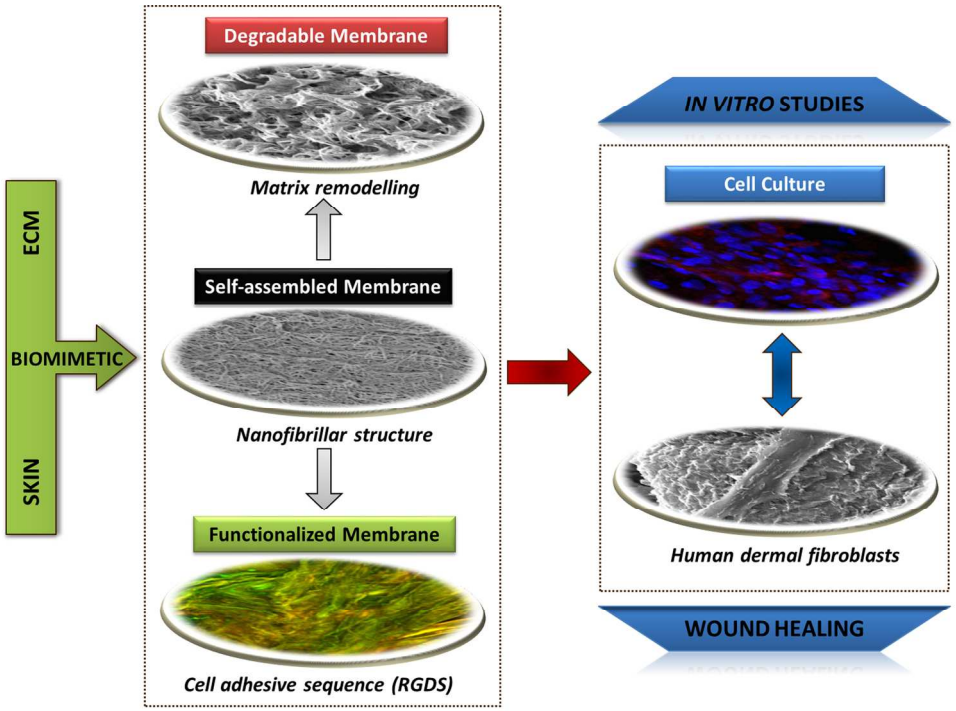

Self-assembled biomimetic membranes presenting different percentages of cell-adhesive ligands for culturing human fibroblasts under serum free conditions.
186x131mm (300 x 300 DPI)

Hyaluronan and self-assembling peptides as building blocks to reconstruct the extracellular environment in skin tissue

Daniela S. Ferreira[1,2], Alexandra P. Marques[1,2], Rui L. Reis[1,2], Helena S. Azevedo[1,2*]

[1] *3B's Research Group - Biomaterials, Biodegradables and Biomimetics, University of Minho, Headquarters of the European Institute of Excellence on Tissue Engineering and Regenerative Medicine, AvePark, 4806-909 Taipas, Guimarães, Portugal*

[2] *ICVS/3B's - PT Government Associate Laboratory, Braga/Guimarães, Portugal*

*corresponding author: hazevedo@dep.uminho.pt

Tel:+351 253 510 907, Fax: +351 253 510 909

Abstract

Self-assembling bioactive membranes, incorporating structural components of skin extracellular matrix (ECM), hyaluronan, and biochemical signaling presenting peptide amphiphiles, for recapitulating some aspects of skin tissue microenvironment, are proposed in this work. In the presented strategy, the availability of cell-adhesion ligands (0-50% RGDS epitope) within 2D membranes is controlled aiming at mastering the adhesion of human dermal fibroblasts under serum-free culture conditions. The membranes were characterized with respect to their microstructure by scanning electron microscopy (SEM), degradability and cell behavior regarding adhesion, proliferation, cytoskeleton organization and epitope distribution. SEM of the membrane surface showed a network of nanofibers that are remarkably reminiscent of the filamentous structure found in the ECM. Confocal microscopy images, using a fluorescently labeled RGDS-peptide, showed that the RGDS signal is uniformly distributed on the membranes. Degradation studies indicated that the membranes are

susceptible to enzymatic degradation by hyaluronidase. In the presence of the enzyme at physiological concentration, the membranes degrade gradually over time. When grown on membranes with the cell recognition epitope RGDS, fibroblasts had spread out and elongated, exhibiting extended filopodia interacting with fibrillar structure of the membrane surface, thus showing improved adhesion to the substrate. This study demonstrates the positive effect of the RGDS epitope, presented on a self-assembled membrane, in promoting cell-matrix interactions.

Keywords: hyaluronan, peptides, self-assembly, membranes, fibroblasts, skin

1. Introduction

The extracellular matrix (ECM) of tissues is a dynamic and hierarchically organized composite structure of various fibrillar proteins and glycosaminoglycans. This network not only has a structural role, providing support and tensile strength for tissues and acting as scaffolds for cell adhesion and organization, but also serves as a storage for growth factors, chemokines and cytokines, and as template for tissue morphogenesis and cell differentiation[1-3].

In skin, the ECM is the largest component of the dermal layer, being composed by structural proteins, like elastin that confers skin elasticity, and collagens, primarily type I and III, which provide structure, strength and integrity[4]. Cell-adhesive proteins like fibronectin, laminin and vitronectin are also present in skin ECM. These glycoproteins have the capacity to bind to cells, via integrins, and to other components of the ECM, namely to glycosaminoglycans, excepting hyaluronan (HA), which is one of the major ECM components in skin[4-5]. HA is an extremely large polymer made up of N-acetylglucosamine and glucuronic acid disaccharide repeating unit (Fig. 1A). High molecular weight HA acts as an ECM organizer which concentrates and organizes the assembly of other proteins in the ECM by providing a macromolecular template, thus contributing to tissue architecture and function during homeostasis[6-7]. These properties confer HA many unique advantages as a starting material for skin regeneration applications.

Cell adhesion to native ECM is mediated through binding of integrin proteins on the cell surface and specific epitopes present on proteins of the ECM, creating a focal adhesion, responsible for anchoring the cell and the communication between cell cytoskeleton and the surrounding environment[8]. One of ECM cell adhesive proteins,

fibronectin, binds to integrins through a domain containing Arg-Gly-Asp-Ser (RGDS)[9]. This sequence, first proposed by Pierschbacher and Rouslahti, functions as a general cell adhesive sequence[10] and has been widely used in biomaterials functionalization, including HA-based hydrogels[11-13], improving cell adhesion and subsequent proliferation[14-17].

Peptides represent an interesting family of building blocks which can self-assemble to create a large number of nanostructures, such as micelles, vesicles and nanofibers[18-20]. Thus, by self-assembly, structurally simple building blocks can be easily gathered to create functionally complex materials[8].

Bottom-up approaches based on the self-assembly of small molecules provide a unique set of advantages to create biomaterials as they offer the possibility of controlling the architecture, shape and dimensions of the bioactive nanostructures, as well as the spatial display and density of the bioactive signals [21]. The architectural resemblance of self-assembled nanofibers to filamentous structures found in natural ECMs represents an additional feature to attain superior biomimetic scaffolds, and a clear advantage in biomaterials engineering.

The fabrication of artificial ECMs can be used to mimic the properties of native tissues as well as to reconstruct cellular microenvironments *in vitro*. We address this challenge by combining self-assembling peptides (peptide amphiphiles) integrating biochemical signals (RGDS ligand) to permit cell adhesion and spreading, and functional molecules (HA), as components of our matrix. These components were shown to self-assemble in 2D membranes[22-24]. Through self-assembly, epitope spatial organization can be controlled at the micrometer and nanometer scales to guide cellular behavior. Materials that selectively interact with cells may be helpful in improving our

understanding of key structural and biochemical ECM components, and ultimately, harnessing the presentation of specific cues to cells. This represents a simplified approach to deconstruct the skin niche and to identify the effect of individual niche components over cell behavior.

2. Materials and methods

Hyaluronan (HA) and fluorescein HA

The hyaluronan used in all experiments had an average molar mass of 2 MDa and was purchased from Lifecore Biomedical, Inc (Chaska, USA). HA was fluorescently labeled with fluoresceinamine (Fig. 3B) using *N*-(3-dimethylaminopropyl)-*N*'-ethylcarbodiimide hydrochloride (EDC) chemistry and following the procedure described by Gajewiak et al.[25]. Briefly, HA (50 mg) was dissolved in 20 mL of water to give a 0.25% (w/v) solution, which was then mixed with a solution of 5 mg of fluoresceinamine (Sigma, USA) in 20 mL of dimethylformamide. Next, 100 mg of N-hydroxysuccinimide (NHS, Sigma, USA) was added, and the solution pH was adjusted to 4.75 with 0.01 M HCl. Finally, 50 mg of EDC (Sigma, USA) was mixed maintaining the solution pH at 4.75. After 12 h, the solution was transferred to dialysis tubing (2000 Da MWCO, Sigma, USA)) and dialyzed exhaustively against 100 mM NaCl, followed by dialysis against distilled water and lyophilization.

Peptide amphiphiles synthesis and purification

Three different peptide amphiphiles (PAs) were synthesized in this work, consisting of a peptide segment covalently linked to a 16-carbon alkyl chain: $C_{15}H_{31}CO$-$V_3A_3K_3$ (K_3-PA, filler), $C_{15}H_{31}CO$-$V_3A_3K_3RGDS$ (K_3RGDS-PA) and $C_{15}H_{31}COV_3A_3K_3DGSR$ (K_3DGSR-PA, scrambled) (Fig.1). The peptides were synthesized on a CS Bio 136XT automated peptide synthesizer (CS Bio, USA) using standard 9-fluorenylmethoxycarbonyl (Fmoc) based solid phase chemistry on a 4-methylbenzhydrylamine (MBHA) rink amide resin. Amino acid couplings were performed using 4 equivalents (4 mmol) of Fmoc protected amino acids (Novabiochem®), 4 equivalents of O-(Benzotriazol-1-yl)-N,N,N',N'-

tetramethyluronium hexafluorophosphate (HBTU, Novabiochem®) and 6 equivalents of N,N-diisopropylethylamine (DIEA, Sigma, USA). Fmoc deprotections were performed with 20% piperidine (Sigma, USA) in dimethylformamide. A palmitic acid ($C_{16}H_{32}O_2$) tail was manually coupled under the same conditions as the Fmoc-amino acids. Peptide cleavage from the resin and removal of the protecting groups was carried out on a mixture of trifluoroacetic acid (TFA, Sigma, USA)/triisopropylsilane (TIS, Alfa Aesar)/water (95/2.5/2.5)) for 3 h at room temperature. The peptide mixture was collected and excess TFA was removed by rotary evaporation. The resulting viscous peptide solution was triturated with cold diethyl ether. The white precipitate was collected by filtration, washed with cold ether, and allowed to dry under vacuum overnight. The peptide mass was confirmed by electrospray ionization mass spectrometry (ESI-MS, Thermo Electron Corporation Finnigan LXQ MS Waltham, USA). Peptides were then purified on a Waters 2545 Binary Gradient high-performance liquid chromatography (HPLC) system using a preparative reverse-phase C18 column (Atlantis Prep OBD T3 Column, Waters) and a water/acetonitrile (0.1% TFA) gradient. TFA counter-ions were exchanged by sublimation from 0.1 M hydrochloric acid. Finally, the peptides were dialyzed against ultrapure water using 500 MWCO dialysis tubing (Spectrum labs, The Netherlands), and lyophilized. Confirmation of mass and purity was done by ESI-MS and HPLC (Supplementary Information, Fig. S1-S3).

A fluorescent version of K_3RGDS-PA, $C_{15}H_{31}CO$-$V_3A_3K_3K_{rhod}$RGDS (Fig. 3B), was also synthesized to allow examining the availability/distribution of the RGDS motif within and on the surface of the membranes. For that, an additional lysine residue, with a 4-Methyl trityl (Mtt) protecting group in the ε amine of the lysine residue (Fmoc-Lys(Mtt)-OH), was introduced in the sequence to which the Rhodamine dye was

attached. The peptide was grown on the resin and after coupling the palmitic tail, the Mtt protecting group was selectively removed with a solution of TFA/TIS/DCM (4:4:92) at room temperature. Resin was incubated with deprotection solution for 5 minutes and washed thoroughly with DCM. These steps were repeated until the resin no longer turned yellow. Then, peptide-resin (150 mg) was swollen in 1150 µL of DMF and 50 µL of DIEA. Ten milligrams of 5-(and 6)-carboxytetramethylrhodamine succinimidyl ester (NHS-rhodamine) were dissolved in the supernatant from the beads swelling step and added to the resin. The reaction took place at room temperature, overnight, and protected from light. After repeatedly washes with DMF and methanol, the peptide was cleaved from the resin following the procedure described above for the other peptides, and purified by HPLC. Mass was confirmed by matrix assisted laser desorption/ionization mass spectrometry (MALDI-MS, 4800 MALDI-TOF/TOF, AbSciex) (Supplementary Information, Fig. S4).

Peptide amphiphiles characterization

Circular dichroism (CD) spectroscopy

Peptides were dissolved in deionized water to a final concentration of 0.033 mM and the pH was adjusted to 5, 7 and 9. The CD measurements were performed in a PiStar-180 spectrometer from Applied Photophysics (Surrey, UK), under a constant flow of nitrogen (8 $L.min^{-1}$) at a constant pressure value of 0.7 MPa. Far-UV spectra were recorded at 25 ºC from 190 to 300 nm in a quartz cuvette with 1 mm path-length. All scans were performed in the steady state with a bandwidth of 1 nm and each represented spectrum is an average of 5 spectra.

Transmission electron microscopy (TEM)

Samples for TEM analysis were prepared by placing a drop of 0.1 mM peptide solution directly on the 400 mesh carbon-coated copper TEM grid (Ted Pella, USA). For negative staining a drop of 2% (w/v) uranyl acetate aqueous solution was placed on the samples. After ca. 3 minutes, the excess solution was wiped away by a piece of filter paper, and the sample was allowed to dry under ambient conditions. All images were collected with a JEOL JEM-1010 transmission electron microscope at 100 kV (JEOL, USA).

Characterization of PA-HA interactions

Quartz crystal microbalance with dissipation (QCM-D)

Measurements were performed in a quartz crystal microbalance with dissipation monitoring (QCM-D E4) from Q-Sense (Gothenburg, Sweden). All the experiments were performed at 25 ºC with a constant flow rate of 50 μl/min using gold coated crystals (QSX301, Q-Sense, Goteborg, Sweden) previously cleaned with water and H_2O_2 for 1 h each, and then acetone, ethanol and isopropanol for 3 minutes each at 37 ºC with sonication. The system was equilibrated with a 0.15 M sodium chloride (NaCl) solution to obtain a stable frequency and dissipation baseline signal. Once the signal was stable, the NaCl solution was replaced by a solution of K_3-PA (0.2% (w/v) in 0.15 M NaCl) during 30 minutes. To remove weakly bound peptide, the crystals were rinsed with a NaCl solution and then replaced by a solution of HA (0.1% (w/v) in 0.15 M NaCl) for 30 minutes. Again, to remove weakly bound polymer, the system was rinsed with NaCl. The QCM instrument recorded frequencies up to the 13^{th} overtone, and Δf and ΔD were monitored in real time. In the present study the results are shown for the 7^{th}

overtone, the frequency of this overtone was normalized to the fundamental resonant frequency of the quartz crystal, by dividing it by v (where $v = 7$).

PA-HA membrane preparation

PA-HA membranes were prepared using a 48 well plate as template in a sterile environment. 150 µL of a 1% (w/v) HA solution was cast on the bottom of the wells and then 150 µL of a 2% (w/v) K_3-PA solution was added on top of the HA solution. A membrane is immediately formed upon contact between the two solutions. The membrane was allowed to grow with time (overnight) as reported previously[23]. The membranes were rinsed with sterile ultrapure water to ensure the removal of unreacted HA and PA.

PA-HA membrane characterization

Scanning electron microscopy (SEM)

The microstructure of the membranes was analyzed by SEM. Samples were fixed in a 2% glutaraldehyde/3% sucrose in PBS for 1 h at 4 ºC followed by sequential dehydration in graded ethanol concentrations (from 20 to 100%). To remove ethanol, samples were chemically dried in hexamethyldisilazane (HMDS, Electron Microscopy Sciences, USA) 3 times, 15 minutes each, and HMDS excess allowed to evaporate. Prior observation, the samples were coated with a gold/palladium layer and imaged using an ultra-high resolution field emission gun scanning electron microscope (Nova™ NanoSEM 200) from FEI (Eindhoven, The Netherlands).

Confocal microscopy

Confocal microscopy was used to probe the location and retention of fluorescently-labeled HA as well as to visualize the distribution of RGDS signal on (surface) and within (cross-section) the PA-HA membrane. Membranes were formed as previously described using fluorescein HA solution (1%, w/v) and 2% (w/v) peptide mixture containing 0.1% of K_3K_{rhod}RGDS-PA and 99.9% of K_3-PA. The membranes were incubated overnight at RT protected from light. After washing, membranes were transferred to glass microscopy slides, covered with a glass coverslip, and sealed to prevent dehydration. Membranes were imaged by laser scanning confocal microscope (LSCM, Olympus FluoView 1000, Japan) with the appropriate excitation and emission wavelengths. Optical slices were captured at regular intervals to produce reconstructed z-stacks with 100 μm total thickness. Images of cross sections were compiled from z-stack in the x-direction using FV10-ASW software from Olympus.

In vitro enzymatic degradation

Degradation behavior of the PA-HA membranes in the absence and presence of a HA-degrading enzyme (hyaluronidase, HAase) was analyzed *in vitro*. Bovine testicular HAase (Type IV, EC 3.2.1.35) was obtained from Sigma (USA). This enzyme has the ability to hydrolyze β(1,4) glycosidic bonds between N-acetyl-D-glucosamine and D-glucuronate residues producing HA fragments with a N-acetyl-D-glucosamine at the reducing end. The enzyme activity can thus be measured by the quantification of these reducing ends. Degradation studies were carried out by incubating PA-HA membranes in PBS at 37 ºC in the absence (control) or presence of HAase at different concentrations, 2.6 U/mL HAase (to simulate physiological conditions in human plasma) and 50 U/mL HAase, for 14 days. The enzyme solution was replaced every 72 h

throughout the study and stored frozen until analysis. At predetermined time points, the solution was completely collected for further quantification of N-acetylamino sugars using the fluorimetric Morgan-Elson assay method[26]. A calibration curve of N-acetyl-D-glucosamine (NAG) standards was used. HA fragments resulting from enzymatic hydrolysis were identified by mass spectrometry in the negative mode (Thermo Electron Corporation Finnigan LXQ MS Waltham, USA). The morphology of the membranes after degradation was analyzed by SEM.

Cell culture studies

Isolation and culture of human primary fibroblasts

Human dermal fibroblasts (hDFb) were isolated from skin samples discarded from abdominoplasty surgeries of consenting patients at Hospital da Prelada (Porto, Portugal). Briefly, the skin tissue was cut in pieces of 0.5 by 0.5 cm and digested in a dispase solution (2.4 U/mL in PBS) at 4 ºC, overnight. After removing the epidermis, the fibroblasts were isolated from the dermis by overnight digestion of the dermal pieces in a collagenase IA solution (125 U/mL in PBS) at 4 ºC. Digestion products were poured through a 100 µm cell strainer and centrifuged at 200 *g* for 5 minutes. The pellet was resuspended and the cells were subsequently cultured in Dulbecco's Modified Eagle Medium (DMEM) (Sigma, Germany) supplemented with 10% of fetal bovine serum (FBS, Gibco, UK) and 1% (v/v) antibiotic/antimycotic solution (A/B) (Gibco, UK) containing 100 units/mL penicillin and 100 mg/mL streptomycin, in a 37 ºC humidified atmosphere with 5% CO_2.

hDFb culture on the PA-HA membranes

To study the effect of RGDS signaling on cell adhesion, PA-HA membranes containing different percentages of RGDS motif were prepared by mixing the filler peptide (K_3-PA) with 1%, 10% and 50% K_3RGDS-PA and 10% scrambled peptide (K_3DGSR-PA) to give a 2% (w/v) final peptide concentration. HA sterilization for cell studies was done by dissolving the polymer, filtering the solution through a 0.22 µm filter, followed by lyophilization in sterile falcon tubes. Peptide solutions were sterilized by UV exposure for 15 minutes. Membranes were prepared following the procedure previously described under sterile conditions. Confluent hDFbs, at passage 4, were harvested from monolayer cultures using trypsin-EDTA (Invitrogen, USA). Cells were washed in PBS and centrifuged at 200 *g* for 10 minutes in order to remove serum residues. Cell pellet was then resuspended at a density of 5.0 x 10^4 cells/mL in serum-free DMEM without phenol red (Sigma, Germany) supplemented with 1% (v/v) A/B. Cells (2.5 x 10^4cells/well) were cultured on the PA-HA membranes in 48 well plates at 37 ºC in a humidified atmosphere of 5% CO_2 for 2, 6, 12 and 24 h. hDFbs cultured on tissue culture polystyrene (TCPS) coverslips were used as control. Cells cultured on the membranes were examined under SEM to analyze cell morphology and cell-matrix interactions. Cell cultured membranes were fixed, dehydrated and prepared as described for SEM analysis.

F-actin staining

Staining for the F-actin cytoskeleton fibers of attached hDFbs was carried out after fixing cells in 10% formalin solution neutral buffer (Sigma-Aldrich, Germany) for 30 minutes at 4 ºC. Cells were then washed once with 0.1 M Glycine in PBS and twice with PBS and permeabilized with 2% BSA/ 0.2% Triton X-100 solution for 1 h at RT. Samples

were incubated with TRITC-conjugated phalloidin (1U/mL, Sigma-Aldrich, Germany) for 1 h at RT. Cell nuclei were counterstained with 1 mg/mL DAPI (1:1000, Sigma-Aldrich, Germany) for 1 min and washed with PBS. Visualization was performed by CLSM (Olympus FluoView 1000, Olympus, Japan). Background was subtracted and images were processed using ImageJ software (NIH, USA).

dsDNA quantification

The number of cells adherent to the membranes was assessed at different culture times by quantifying the amount of double-stranded DNA (dsDNA). Quantification was performed using the Quant-iT™ PicoGreen® dsDNA Assay Kit (Invitrogen, Molecular Probes, Oregon, USA), according to the instructions of the manufacturer. Briefly, cells on the different membranes were lysed by osmotic and thermal shock and the supernatant used for the DNA quantification. The fluorescent intensity of the dye was measured in a microplate reader (Synergie HT, Bio-Tek, USA) with excitation at 485/20 nm and emission at 528/20 nm. The DNA concentration for each sample was calculated using a standard curve (DNA concentration ranging from 0 to 1.5 mg/mL) relating quantity of DNA and fluorescence intensity. Triplicates were made for each time point and for each sample.

Data analysis and statistics

Statistical analysis for NAG and DNA quantification was performed using the non-parametric Kruskal-Wallis test, after testing the normality of our data with Shapiro-Wilk test. Dunn's post-hoc test were carried out to determine the differences between

the various conditions under this study. Values of $p < 0.05$ were considered to determine statistically significant differences between the groups.

3. Results and discussion

Peptide design and formulation in the bioactive membranes

The self-assembling peptides used in this study are amphiphilic peptides consisting in a linear hydrophobic segment coupled to a peptide sequence, that includes a β-sheet forming sequence (VVVAAA) and a domain with positively charged amino lysines (KKK) to bind the anionic HA (K_3-PA). This class of self-assembling peptides, known as peptide amphiphiles (PAs), was proposed by Stupp's group for different biomedical applications[19, 27-28]. The fibronectin-derived RGDS epitope was incorporated into the peptide structure (K_3RGDS-PA) due to its known properties on mediating cell adhesion (Fig. 1A). Different PA molecules have been co-assembled, allowing for a specific bioactive molecule to be mixed with a non-bioactive diluent molecule[29-32] to vary the epitope density on the assembled structures for optimized cell signaling. For example, Webber and co-workers[29] have investigated the co-assembly of a positively charged PA containing the RGDS sequence (K_3RGDS-PA) with negative diluent PA (E_3-PA) with the aim of producing mixed binary nanofibers. By varying the RGDS composition on surfaces coated with the co-assembled peptide nanofibers, they were able to determine the optimal RGDS density on the adhesion of bone-marrow mononuclear cells. While this co-assembly strategy has been explored by other groups, using coated surfaces[29, 31] or self-assembled gels[32], the co-assembly of RGDS-containing peptides with HA in self-assembled membranes has been explored by our group[33]. In this configuration, the membranes present different densities of biomolecular signals designed to enhance cell adhesion, but other biochemical functionalities can be incorporated, like growth-factor binding sequences relevant in wound healing.

Previous studies have shown that the formation of stable β-sheet is very important and necessary for peptide self-assembly[20, 34]. Although the formation of β-sheet secondary structure of K_3-PA has been demonstrated previously[35], the inclusion of the RGDS (or DGSR) in the PA sequence could disturb that rearrangement and consequently affect the stability of self-assembled membranes. Therefore, circular dichroism (CD) spectroscopy was performed to evaluate the secondary structure of the synthesized peptides (Fig. 1B). The CD analysis of the PAs revealed the presence of hydrogen-bonded structures, namely β-sheets or random coil, depending on the pH. At pH 9, a typical spectrum of β-sheet structure was observed for all the molecules, with a minimum in the 210-220 nm range, a crossover from positive to negative above 190 nm, and a positive ellipticity around 200 nm. The scrambled peptide showed this conformation in all the studied pH conditions, with stronger peaks at 205 nm. Below pH 9, the K_3RGDS-PA showed a random coil conformation. K_3-PA presented a β-sheet structure with a minimum at 220 nm and a maximum at 205 nm at pH 7, and a random coil conformation at pH 5. TEM analysis showed the formation of nanofibers for all the peptides, but K_3DGSR-PA formed shorter fibers than the K_3 and K_3RGDS-PAs (Fig. 1C).

PA-HA interaction

Previous studies have shown the ability of K_3-PA to interact with HA and form macroscopic structures, such sacs and membranes, by self-assembly[22-24]. In the herein presented work, we have investigated, for the first time, the interactions between these two molecules by QCM-D. This technique allows marker-free measurement of specific interactions between immobilized molecules and analytes in solution and has been widely used for studying macromolecular interactions. Due to its sensitivity,

allows detecting mass changes of the order of ng.cm^{-2}, and permits to measure the viscoelastic properties of the resulting film[36-37]. Figure 2 shows the normalized frequency ($\Delta f_v/v$, where v is the overtone) and dissipation (ΔD) variations for the 7th overtone (35 MHz). The first 15 minutes in Figure 2 show the establishment of the baseline with 0.15 M NaCl. The subsequent 45 minutes correspond to the deposition of K_3-PA, where a decrease in the frequency (of about 23 Hz) and an increase in ΔD were observed. After rinsing with NaCl, the hyaluronan solution was pumped continuously for 45 minutes, when an adsorption plateau was attained. A decrease in frequency of 38 Hz was registered, and again an increase in dissipation has occurred. After HA deposition, the film was again rinsed with NaCl. During this washing step, the variation in both Δf and ΔD was very small, indicating the formation of a stable film and a strong interaction between both molecules. The frequency variation, Δf, decreases with time, due to the deposition of peptide or hyaluronan on the quartz crystal. On the other hand, the dissipation, ΔD, increases, revealing that the film is not rigid and begins dissipating energy, thus exhibiting the typical viscoelastic behavior. This behavior has been observed before when studying the interaction between poly(L-lysine) and hyaluronan by QCM-D[38]. The QCM-D results demonstrated and confirmed the strong interaction between the K_3-PA and HA and the formation of stable complex.

Membrane microstructure and degradation

In this work, we aimed to recreate some aspects of the physical and biochemical environment of skin tissue. It was shown previously that hierarchical membranes can be formed by instant self-assembly between a positively charged PA (K_3-PA) and the

megadalton hyaluronan (HA) under certain conditions[22-23]. We thought that these fibrillar membranes, containing components of skin ECM, could provide a starting platform to design complex biomimetic environments of skin ECM (Fig. 3). SEM analysis of the microstructure of the membranes revealed a very highly organized structure exhibiting two distinct surfaces, as observed previously[22-23, 32]. The surface corresponding to the HA side (Fig. 3C1) is characterized by a rough and amorphous structure, whereas the peptide side (Fig. 3C2), exhibit a network of organized nanostructures (nanofibers) randomly distributed, resembling the fibrillar structure of natural ECM. SEM micrographs of the cross section revealed a membrane with around 14 µm in thickness and aligned nanofiber bundles perpendicular to the interface (Fig. 3C3). To investigate if the addition of the K_3RGDS-PA would affect the membrane microstructure and morphology, SEM was used to image membranes containing 50% K_3RGDS-PA. Membranes containing 50% of K_3RGDS-PA presented a similar thickness and microstructure to the ones formed with 100% of K_3-PA (Fig. S5, supplementary information). Fluorescent micrographs obtained by confocal microscopy, using the fluorescently labeled K_3K_{rhod}RGDS-PA (red) and hyaluronan (green), showed a perfect overlap of the two, in yellow, resulting from the interaction between the peptide and hyaluronan (Fig. 3B2). This strong yellow region is also seen in a software simulated cross section (Fig. 3B1), surrounded by a soft area in red or green, that correspond to the peptide and hyaluronan side, respectively. The uniform distribution of the red signal showed that RGDS molecules were well distributed within the membranes although the spatio control of the signal on specific locations of the membrane is yet a major challenge.

The natural ECM is an extremely dynamic network that consists of protein fibers and glycosaminoglycans that support cell fate and provide biophysical and biochemical cues to cells through cell surface receptors, such as integrins[1-2, 39]. Cells degrade the ECM through proteases during their migration. Synthetic ECM matrices that aim to provide an environment for tissue regeneration should recapitulate key features of the natural ECM such as integrin mediated cell binding, cell migration, and cell proliferation, while also allowing their degradation, offering a platform on which cell-triggered remodeling could occur. To mimic the turnover of natural ECM, our matrices were designed to be sensitive to enzymes expressed by surrounding cells (e.g. hyaluronidase). This cell-mediated degradation is a process reminiscent of tissue remodeling. It is well known that the degradation of hyaluronan into large oligosaccharides is mediated by hyaluronidase[40]. Therefore, the degradation behavior of the PA-HA membranes was studied in three different conditions, PBS and PBS containing 2.6 U/mL and 50 U/mL HAase. Degradation was followed by the quantification of N-acetylglucosamine in solution and by SEM analysis (Fig. 4). Incubation in PBS up to 14 days did not cause degradation of the membranes since the amount of N-acetylamino sugars in the supernatant was significantly lower than the obtained for the membranes incubated in the higher enzyme concentration (50 U/mL). Compared with the physiological concentration (2.6 U/mL), only for the latest time point a statistically difference was observed. In addition, no evident signs of degradation are observed in the SEM images for the membranes incubated in PBS only. This result indicates that the membranes are relatively stable in buffer saline solutions, but are susceptible to enzymatic degradation by HAase. As expected, the membrane degradation was significantly enhanced when incubated with higher

enzyme concentration (50 U/mL) than when in presence of the enzyme at physiological conditions (2.6 U/mL), as demonstrated by the higher amount of released N-acetylamino sugars (Fig. 4A). SEM analysis of the membranes collected at different time points corroborates these results, showing the appearance of pores on the membrane surface (Fig. 4B1) and cross-section (Fig. 4B2), as a result of HA degradation by HAase. At a higher HAase concentration (50 U/mL) the degradation of the membranes is more evident, but progressive along the time (Fig. 4B1-B2).

The presence of HA oligosaccharides as degradation products was confirmed by mass spectroscopy. ESI-MS analysis of the supernatants after membrane degradation in 2.6 U/mL HAase solution for 7 days showed three main peaks, corresponding to $[HA]_{11}$: $[M-2H]^{2-}$ m/z= 1046.25, $[HA]_{12}$: $[M-2H]^{2-}$ m/z= 1142 and $[HA]_{14}$ $[M-2H]^{2-}$ m/z= 1332.17 (Fig 4C)[41]. The observed mass for $[HA]_{11}$ is a fragmentation product of ESI-MS since digestion with HAase produces even-numbered oligosaccharides. To confirm that the observed masses are not caused by the technique itself ESI-MS analysis was performed of a HA solution (Fig. S6, supplementary information) but no known masses of HA oligosaccharides were identified.

The membranes herein presented were shown to degrade gradually over time in the presence of HAase at physiological concentration. In addition, it is expected that the peptide component of the membrane will degrade overtime by hydrolytic and enzymatic processes into amino acids, which are nontoxic and easily cleared in the body. Peptides can be designed to be susceptible to enzymatic cleavage by incorporating matrix metalloproteases (MMPs)-sensitive peptide sequences[42-43], a strategy that is currently being explored in our lab. By having membranes sensitive to enzymatic activities, we are pursuing the goal of biomimetic matrix degradation. These

PA-HA membranes may present an advantage over other systems, once slow degradation will enable the migration of the adhered cells, as well as matrix remodeling and new tissue formation led by the artificial ECM template

Fibroblast response to the PA-HA self-assembled membranes displaying different densities of the RGDS epitope

Preliminary studies were performed with hDFb cultured on K_3PA-HA membranes in DMEM with 10% FBS up to 7 days. These studies indicated that these membranes supported the adherence of fibroblasts, without presenting cytotoxicity (Fig. S7, supplementary information).

Understanding the factors that regulate cell behavior is important in many therapeutic applications. In most studies, cell behavior is studied in culture medium supplemented with serum, which is poorly defined in terms of proteins content. To investigate whether the produced PA-HA membranes could integrate cell-adhesive ligands and anchor human dermal fibroblasts, serum-free culture conditions were used to eliminate the complexity of the competing adsorption process of serum proteins on the membrane surface.

It has been shown that fibroblast survival, proliferation and migration are dependent on cell adhesion and that fibronectin (FN) binding domains have significant implications on skin wound healing[4]. These activities require fibroblast attachment to RGD sequence in the tenth FN type III repeat, via cell surface membrane integrin receptors[44]. Several authors reported that inert biomaterials benefit from the presence of the RGDS signaling molecule for optimal cell recognition and adhesion[14-16, 31]. To enhance the adhesion of cells on the developed PA-HA membranes, the RGDS motif

(which is a known ligand for integrin receptors) was incorporated into the PA structure creating adhesion points to support integrin-mediated cellular adhesion and migration on the membranes. Previous studies have shown that the density of the RGDS epitope impacts cell recognition and adhesion[45]. Considering this, experiments were performed varying the K_3RGDS-PA composition on the membranes (1, 10 and 50%) to determine the optimal RGDS density. Membranes containing 10% K_3DGSR-PA or only K_3-PA were used as controls.

DNA quantification results (Fig. 5A) showed that when seeded on 50% K_3RGDS-PA containing membranes, hDFb adhered at significantly higher number than on the ones with lower concentration of RGDS, 1 and 10%, or without RGDS, K_3-PA and K_3DGSR-PA for all time points except at 12h of culture.

Cell morphology and distribution on the membranes was further examined by confocal microscopy analysis (Fig. 5B). After the first two hours, fibroblasts were uniformly distributed on the membrane surface and a high number of cells was observed on the 50% K_3RGDS-PA containing membranes, as depicted by the higher density of nuclei. These results demonstrate the positive effect of the RGDS epitope on promoting cell adhesion which is mediated by integrins on the cell surface. Considering the presence of HA on the membranes and knowing that CD44, a transmembrane receptor observed in a number of different cell types[46], mediates HA dependent cell adhesion, the expression of this receptor by hDFbs was assessed (Supplementary Information, Fig. S8) . Although these cells showed a high expression of CD44 (98.67%), cells cultured on HA-based hydrogels (Supplementary Information, Fig. S9) did not show strong adhesion on these substrates. This result suggest that integrins may play a major role, rather than CD44, on cell adhesion on PA-HA membranes.

Staining of cell cytoskeleton (Fig. 5B) did not reveal strong organized actin fibers. Most of what is known about cell structure and function *in vitro* derives from cells plated on rigid substrates, such as plastic or glass, laminated with a thin film of serum proteins. As a result, some prominent aspects of cell structure, such as the elongated morphology of cultured fibroblasts or the prevalence of large actin fibers that are commonly studied *in vitro*, are rarely if ever seen *in vivo*[47-48]. Furthermore, cells cultured on soft substrates show diffuse adhesion complexes with poor actin cytoskeleton organization[49] and the PA-HA membranes used in this study were shown to have low stiffness (0.9 MPa in the wet state)[23].

Previous findings have also shown that fibronectin fragments containing the RGD cell-binding domain alone cannot sustain cytoskeletal organization of human dermal fibroblasts[50], which might explain our observations.

Fibroblasts morphology observed in the SEM micrographs is similar to what has been observed previously by others on RGD-coated glass substrates[45]. After 24 hours of culture, only the conditions with 10% and 50% K_3RGDS-PA showed the majority of the cells fully adherent (Fig. 6). In these conditions, fibroblasts had spread out exhibiting extended lamellipodia and filopodia interacting with fibrillar structure of the membrane surface, thus confirming strong adhesion to the substrate (Fig. 6a and b). In contrast, cells cultured on the surface of smooth HA hydrogel (Supplementary Information, Fig. S9) were completely round, without showing cell protusions (lamellipodia and filopodia) and did not flatten upon contact with the hydrogel surface. This result highlights the role of the nanofibrillar structure of the self-assembled membranes in controlling cell-matrix interactions. This is in accordance to what was reported in the literature, that fibroblasts in 2D cultures normally exhibit a flat

morphology with dorsal-ventral polarity and large lamellipodia[51]. We should highlight that the cell culture experiments were performed in the absence of serum for the entire study and the membranes are displaying the RGDS cell-adhesive domain alone. Further experiments are yet needed to investigate cell response to HA-PA membranes with higher stiffness and/or with other fibronectin fragment domains in order to be able to make additional considerations regarding the effect of each one of these variables over cell morphology.

4. Conclusion

This study demonstrated that the 2D membranes, formed by self-assembly between hyaluronan and a positively charged peptide amphiphile, are susceptible to enzymatic degradation by hyaluronidase. In the presence of hyaluronidase at physiological concentration, the membranes slowly degrade overtime. The gradual degradation of the membranes is important for allowing the migration of cells and/or the controlled release of bioactive molecules incorporated in the membrane that can control the function of attached cells. Membranes presenting the cell adhesive ligand RGDS showed to increase efficiently the attachment of fibroblasts. This capability to incorporate biochemical signals into 2D self-assembled membranes enables the study of cellular responses to physiologically relevant signal variations. Furthermore, these bioactive matrices permit cell culture studies without serum for short periods. We expect that the proposed biodegradable hybrid membranes could offer significant potential as a biomimetic bioactive supportive matrix for wound healing.

Acknowledgements

Funding for this study was provided by the Portuguese Foundation for Science and Technology (FCT, grant PTDC/EBB-BIO/114523/2009). D.S. Ferreira gratefully acknowledges FCT for the PhD scholarship (SFRH/BD/44977/2008). We also thank Dr A. M. Azevedo from Instituto Superior Técnico (BERG, Lisbon, Portugal) for her support obtaining circular dichroism data, M. T. Cerqueira and I. M. Martins from the 3B's Research Group at the University of Minho (Portugal) for assistance on the isolation of human dermal fibroblasts and FACS analysis, respectively.

Author contributions

DSF and HSA designed the study; DSF performed the experimental work; DSF and HSA wrote the paper; APM and RLR revised the paper. All authors discussed the results and commented on the manuscript.

5. References

1. H. K. Kleinman, D. Philp, M. P. Hoffman, Role of the extracellular matrix in morphogenesis. *Curr. Opin. Biotechnol.* 2003, *14*. 526-532, DOI: 10.1016/j.copbio.2003.08.002.
2. W. P. Daley, S. B. Peters, M. Larsen, Extracellular matrix dynamics in development and regenerative medicine. *J. Cell Sci.* 2008, *121*. 255-264, DOI: 10.1242/jcs.006064.
3. F. G. Giancotti, E. Ruoslahti, Integrin Signaling. *Science* 1999, *285*. 1028-1033, DOI: 10.1126/science.285.5430.1028.
4. M. S. Agren, M. Werthen, The Extracellular Matrix in Wound Healing: A Closer Look at Therapeutics for Chronic Wounds. *The International Journal of Lower Extremity Wounds* 2007, *6*. 82-97, DOI: 10.1177/1534734607301394.
5. S. Sakai, R. Yasuda, T. Sayo, O. Ishikawa, S. Inoue, Hyaluronan Exists in the Normal Stratum Corneum. 2000, *114*. 1184-1187.
6. D. Jiang, J. Liang, P. W. Noble, Hyaluronan as an Immune Regulator in Human Diseases. *Physiological Reviews* 2011, *91*. 221-264, DOI: 10.1152/physrev.00052.2009.
7. R. Stern, H. I. Maibach, Hyaluronan in skin: aspects of aging and its pharmacologic modulation. *Clin. Dermatol.* 2008, *26*. 106-122, DOI: 10.1016/j.clindermatol.2007.09.013.
8. J. H. Collier, J. S. Rudra, J. Z. Gasiorowski, J. P. Jung, Multi-component extracellular matrices based on peptide self-assembly. *Chem. Soc. Rev.* 2010, *39*. 3413-3424, DOI: 10.1039/b914337h.
9. E. Ruoslahti, M. D. Pierschbacher, Arg-Gly-Asp: A versatile cell recognition signal. *Cell* 1986, *44*. 517-518.
10. M. D. Pierschbacher, E. Ruoslahti, Cell attachment activity of fibronectin can be duplicated by small synthetic fragments of the molecule. *Nature* 1984, *309*. 30-33.
11. Y. D. Park, N. Tirelli, J. A. Hubbell, Photopolymerized hyaluronic acid-based hydrogels and interpenetrating networks. *Biomaterials* 2003, *24*. 893-900, DOI: 10.1016/s0142-9612(02)00420-9.
12. S. Khetan, J. S. Katz, J. A. Burdick, Sequential crosslinking to control cellular spreading in 3-dimensional hydrogels. *Soft Matter* 2009, *5*. 1601-1606, DOI: 10.1039/b820385g.
13. J. A. Burdick, G. D. Prestwich, Hyaluronic Acid Hydrogels for Biomedical Applications. *Adv. Mater.* 2011, *23*. H41-H56, DOI: 10.1002/adma.201003963.
14. U. Hersel, C. Dahmen, H. Kessler, RGD modified polymers: biomaterials for stimulated cell adhesion and beyond. *Biomaterials* 2003, *24*. 4385-4415, DOI: 10.1016/s0142-9612(03)00343-0.
15. J. P. Jung, A. K. Nagaraj, E. K. Fox, J. S. Rudra, J. M. Devgun, J. H. Collier, Co-assembling peptides as defined matrices for endothelial cells. *Biomaterials* 2009, *30*. 2400-2410, DOI: 10.1016/j.biomaterials.2009.01.033.
16. L. Perlin, S. MacNeil, S. Rimmer, Production and performance of biomaterials containing RGD peptides. *Soft Matter* 2008, *4*. 2331-2349, DOI: 10.1039/b801646a.
17. K. Shroff, E. L. Rexeisen, M. A. Arunagirinathan, E. Kokkoli, Fibronectin-mimetic peptide-amphiphile nanofiber gels support increased cell adhesion and promote ECM production. *Soft Matter* 2010, *6*. 5064-5072, DOI: 10.1039/c0sm00321b.
18. X. Zhao, F. Pan, H. Xu, M. Yaseen, H. Shan, C. A. E. Hauser, S. Zhang, J. R. Lu, Molecular self-assembly and applications of designer peptide amphiphiles. *Chem. Soc. Rev.* 2010, *39*. 3480-3498.
19. H. Cui, M. J. Webber, S. I. Stupp, Self-assembly of peptide amphiphiles: From molecules to nanostructures to biomaterials. *Peptide Science* 2010, *94*. 1-18, DOI: 10.1002/bip.21328.
20. D. W. P. M. Lowik, J. C. M. van Hest, Peptide based amphiphiles. *Chem. Soc. Rev.* 2004, *33*. 234-245.
21. S. G. Zhang, Fabrication of novel biomaterials through molecular self-assembly. *Nat. Biotechnol.* 2003, *21*. 1171-1178, DOI: 10.1038/nbt874.

22. D. Carvajal, R. Bitton, J. R. Mantei, Y. S. Velichko, S. I. Stupp, K. R. Shull, Physical properties of hierarchically ordered self-assembled planar and spherical membranes. *Soft Matter* 2010, *6*. 1816-1823, DOI: 10.1039/b923903k.
23. R. M. Capito, H. S. Azevedo, Y. S. Velichko, A. Mata, S. I. Stupp, Self-assembly of large and small molecules into hierarchically ordered sacs and membranes. *Science* 2008, *319*. 1812-1816, DOI: 10.1126/science.1154586.
24. L. W. Chow, R. Bitton, M. J. Webber, D. Carvajal, K. R. Shull, A. K. Sharma, S. I. Stupp, A bioactive self-assembled membrane to promote angiogenesis. *Biomaterials* 2011, *32*. 1574-1582.
25. J. Gajewiak, S. S. Cai, X. Z. Shu, G. D. Prestwich, Aminooxy pluronics: Synthesis and preparation of glycosaminoglycan adducts. *Biomacromolecules* 2006, *7*. 1781-1789, DOI: 10.1021/bm060111b.
26. T. Takahashi, M. Ikegami-Kawai, R. Okuda, K. Suzuki, A fluorimetric Morgan-Elson assay method for hyaluronidase activity. *Anal Biochem* 2003, *322*. 257-63, DOI: S0003269703005347 [pii].
27. J. D. Hartgerink, E. Beniash, S. I. Stupp, Peptide-amphiphile nanofibers: A versatile scaffold for the preparation of self-assembling materials. *Proceedings of the National Academy of Sciences* 2002, *99*. 5133-5138, DOI: 10.1073/pnas.072699999.
28. M. J. Webber, J. Tongers, C. J. Newcomb, K. T. Marquardt, J. Bauersachs, D. W. Losordo, S. I. Stupp, Supramolecular nanostructures that mimic VEGF as a strategy for ischemic tissue repair (vol 108, pg 13438, 2011). *Proc. Natl. Acad. Sci. U. S. A.* 2012, *109*. 9220-9220, DOI: 10.1073/pnas.1207994109.
29. M. J. Webber, J. Tongers, M. A. Renault, J. G. Roncalli, D. W. Losordo, S. I. Stupp, Development of bioactive peptide amphiphiles for therapeutic cell delivery. *Acta Biomater.* 2010, *6*. 3-11, DOI: 10.1016/j.actbio.2009.07.031.
30. R. N. Shah, N. A. Shah, M. M. D. Lim, C. Hsieh, G. Nuber, S. I. Stupp, Supramolecular design of self-assembling nanofibers for cartilage regeneration. *Proc. Natl. Acad. Sci. U. S. A.* 2010, *107*. 3293-3298, DOI: 10.1073/pnas.0906501107.
31. H. Storrie, M. O. Guler, S. N. Abu-Amara, T. Volberg, M. Rao, B. Geiger, S. I. Stupp, Supramolecular crafting of cell adhesion. *Biomaterials* 2007, *28*. 4608-4618, DOI: 10.1016/j.biomaterials.2007.06.026.
32. R. H. Zha, S. Sur, S. I. Stupp, Self-assembly of Cytotoxic Peptide Amphiphiles into Supramolecular Membranes for Cancer Therapy. *Advanced Healthcare Materials* 2013, *2*. 126-133, DOI: 10.1002/adhm.201200118.
33. A. C. Mendes, K. H. Smith, E. Tejeda-Montes, E. Engel, R. L. Reis, H. S. Azevedo, A. Mata, Co-Assembled and Microfabricated Bioactive Membranes. *Adv. Funct. Mater.* 2013, *23*. 430-438, DOI: 10.1002/adfm.201201065.
34. X. M. Wang, A. Horii, S. G. Zhang, Designer functionalized self-assembling peptide nanofiber scaffolds for growth, migration, and tubulogenesis of human umbilical vein endothelial cells. *Soft Matter* 2008, *4*. 2388-2395, DOI: 10.1039/b807155a.
35. H. A. Behanna, J. Donners, A. C. Gordon, S. I. Stupp, Coassembly of amphiphiles with opposite peptide polarities into nanofibers. *J. Am. Chem. Soc.* 2005, *127*. 1193-1200, DOI: 10.1021/ja044863u.
36. R. R. Costa, C. A. Custodio, A. M. Testero, F. J. Arias, J. C. Rodriguez-Cabello, N. M. Alves, J. F. Mano, Stimuli-Responsive Thin Coatings Using Elastin-Like Polymers for Biomedical Applications. *Adv. Funct. Mater.* 2009, *19*. 3210-3218, DOI: 10.1002/adfm.200900568.
37. L. Y. Shen, P. Chaudouet, J. A. Ji, C. Picart, pH-Amplified Multilayer Films Based on Hyaluronan: Influence of HA Molecular Weight and Concentration on Film Growth and Stability. *Biomacromolecules* 2011, *12*. 1322-1331, DOI: 10.1021/bm200070k.
38. C. Picart, P. Lavalle, P. Hubert, F. J. G. Cuisinier, G. Decher, P. Schaaf, J. C. Voegel, Buildup mechanism for poly(L-lysine)/hyaluronic acid films onto a solid surface. *Langmuir* 2001, *17*. 7414-7424, DOI: 10.1021/la010848g.

39. J. A. Hubbell, Materials as morphogenetic guides in tissue engineering. *Curr. Opin. Biotechnol.* 2003, *14*. 551-558, DOI: DOI 10.1016/j.copbio.2003.09.004.
40. B. Smedsrod, Cellular events in the uptake and degradation of hyaluronan. *Adv. Drug Deliv. Rev.* 1991, *7*. 265-278.
41. D. J. Mahoney, R. T. Aplin, A. Calabro, V. C. Hascall, A. J. Day, Novel methods for the preparation and characterization of hyaluronan oligosaccharides of defined length. *Glycobiology* 2001, *11*. 1025-33.
42. K. M. Galler, L. Aulisa, K. R. Regan, R. N. D'Souza, J. D. Hartgerink, Self-assembling multidomain peptide hydrogels: designed susceptibility to enzymatic cleavage allows enhanced cell migration and spreading. *J Am Chem Soc* 2010, *132*. 3217-23, DOI: 10.1021/ja910481t.
43. J. Patterson, J. A. Hubbell, Enhanced proteolytic degradation of molecularly engineered PEG hydrogels in response to MMP-1 and MMP-2. *Biomaterials* 2010, *31*. 7836-45, DOI: S0142-9612(10)00841-0 [pii]

10.1016/j.biomaterials.2010.06.061.
44. F. Lin, X.-D. Ren, Z. Pan, L. Macri, W.-X. Zong, M. G. Tonnesen, M. Rafailovich, D. Bar-Sagi, R. A. F. Clark, Fibronectin Growth Factor-Binding Domains Are Required for Fibroblast Survival. *J Invest Dermatol* 2011, *131*. 84-98.
45. S. P. Massia, J. A. Hubbell, An RGD spacing of 440 nm is sufficient for integrin alpha V beta 3-mediated fibroblast spreading and 140 nm for focal contact and stress fiber formation. *The Journal of Cell Biology* 1991, *114*. 1089-1100, DOI: 10.1083/jcb.114.5.1089.
46. A. Aruffo, I. Stamenkovic, M. Melnick, C. B. Underhill, B. Seed, CD44 is the principal cell surface receptor for hyaluronate. *Cell* 1990, *61*. 1303-13, DOI: 0092-8674(90)90694-A [pii].
47. T. Yeung, P. C. Georges, L. A. Flanagan, B. Marg, M. Ortiz, M. Funaki, N. Zahir, W. Y. Ming, V. Weaver, P. A. Janmey, Effects of substrate stiffness on cell morphology, cytoskeletal structure, and adhesion. *Cell Motil. Cytoskeleton* 2005, *60*. 24-34, DOI: 10.1002/cm.20041.
48. D. A. Lauffenburger, A. F. Horwitz, Cell Migration: A Physically Integrated Molecular Process. *Cell* 1996, *84*. 359-369.
49. D. E. Discher, P. Janmey, Y.-l. Wang, Tissue Cells Feel and Respond to the Stiffness of Their Substrate. *Science* 2005, *310*. 1139-1143, DOI: 10.1126/science.1116995.
50. R. A. F. Clark, J.-Q. An, D. Greiling, A. Khan, J. E. Schwarzbauer, Fibroblast Migration on Fibronectin Requires Three Distinct Functional Domains. 2003, *121*. 695-705.
51. K. M. Yamada, E. Cukierman, Modeling tissue morphogenesis and cancer in 3D. *Cell* 2007, *130*. 601-610, DOI: 10.1016/j.cell.2007.08.006.

Figure 1. Peptide design and characterization. A) Chemical structure of the building blocks used for preparing the self-assembled membranes, hyaluronan (HA) and different peptide amphiphiles (PAs): $V_3A_3K_3$ containing positively charged lysines (KKK) to bind the anionic HA, one containing the RGDS epitope (K_3RGDS-PA), a scrambled version (K_3DGSR-PA). B) Circular dichroism spectra of peptide solutions ($3.3x10^{-5}$ M) at pH 5, 7 and 9 showing predominant β-sheet secondary structure. C) TEM images of PA nanostructures formed by deposition of 0.1 mM solutions in water followed by air drying on a carbon-coated TEM grid.

Figure 2. PA-HA interaction. QCM-D monitoring of frequency (Δf, black) and dissipation (ΔD, red) changes obtained at 7^{th} overtone, during deposition of peptide (step 1) and hyaluronan (step 3) on a bare crystal (step 2 relates to rising). The frequency of this overtone was normalized to the fundamental resonant frequency of the quartz crystal, by dividing it by *v* (where *v* = 7).

Figure 3. PA-HA membrane microstructure. A) Schematic representation of PA-HA membranes functionalized with bioactive molecules (green) interacting with cell integrins (yellow). B) Confocal microscopy images of the membranes prepared with 1% (w/v) fluorescein-HA and 2% (w/v) peptide mixture containing 0.1% K_3K(Rhod)RGDS-PA. Images show the localization of HA (green) and PA (red) over the membrane surface (B2) and cross section (B1). Yellow represents the overlaping of both components. C) SEM micrographs of self-assembled membranes with 1% (w/v) HA and 2% (w/v) K_3-PA, showing the surface on the polymer (C1) and peptide (C2) sides and cross section (C3, C4).

Figure 4. Degradation of PA-HA membranes. A) Quantification of N-acetylamino sugars released from K_3-HA membranes in PBS and PBS containing 2.6 U/mL and 50 U/mL HAase (*$p < 0.05$, error bars represent standard deviation (n=3)). B1) SEM images showing differences in membrane microstructure when exposed to different hyaluronidase (HAase) concentrations up to 14 days. B2) Cross section of the membranes before and after exposure to 50 U/mL HAase evidencing that degradation is occurring not only on the surface but also inside the membrane. C1) Negative ESI-MS

of the supernatant after incubating the membranes in 2.6 U/mL HAase for 7 days showing the presence of HA fragments. C2) Observed and theoretical molecular masses of HA oligosaccharides.

Figure 5. Cell adhesion on PA-HA membranes. dsDNA quantification (A) (*$p < 0.05$, error bars represent standard deviation (n=3)) and confocal fluorescence images (B) of hDFb cultured on HA-PA membranes containing 1, 10 and 50% K_3RGDS-PA or 10% (w/v) K_3DGSR-PA up to 24 hours of culture. F-actin was labeled with TRITC-phalloidin (red) and nuclei with DAPI (blue).

Figure 6. Cell morphology on PA-HA membranes. A) SEM micrographs of hDFb cultured on HA-PA membranes containing 1, 10 and 50% K_3RGDS-PA or 10% (w/v) K_3DGSR-PA. Cells were cultured on the PA side in medium without FBS up to 24 h. a) and b) show a higher magnification of the surfaces of HA-PA membranes with 10 and 50% (w/v) RGDS, respectively. Black and white arrows indicate the presence of filopodia and lamellipodia, respectively.

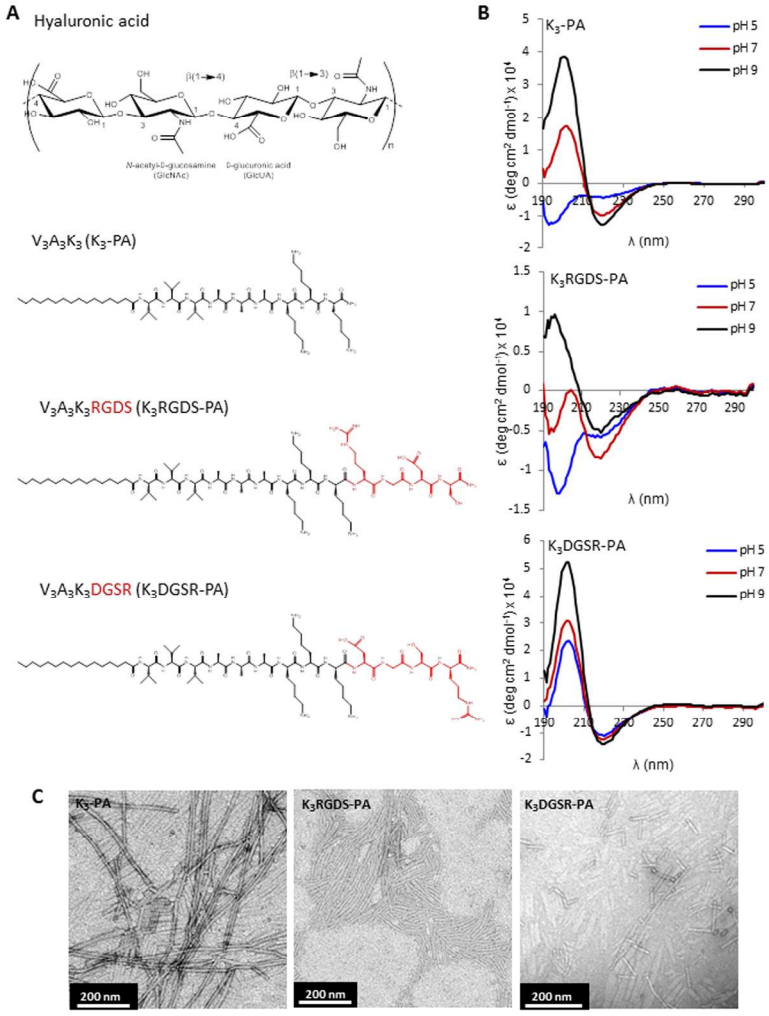

Figure 1. Peptide design and characterization. A) Chemical structure of the building blocks used for preparing the self-assembled membranes, hyaluronan (HA) and different peptide amphiphiles (PAs): V3A3K3 containing positively charged lysines (KKK) to bind the anionic HA, one containing the RGDS epitope (K3RGDS-PA), a scrambled version (K3DGSR-PA). B) Circular dichroism spectra of peptide solutions (3.3x10-5 M) at pH 5, 7 and 9 showing predominant β-sheet secondary structure. C) TEM images of PA nanostructures formed by deposition of 0.1 mM solutions in water followed by air drying on a carbon-coated TEM grid.
275x397mm (300 x 300 DPI)

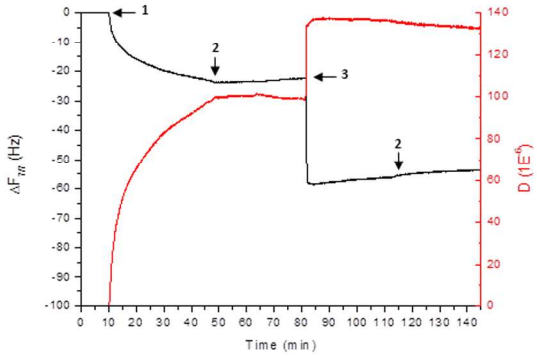

Figure 2. PA-HA interaction. QCM-D monitoring of frequency (Δf, black) and dissipation (ΔD, red) changes obtained at 7th overtone, during deposition of peptide (step 1) and hyaluronan (step 3) on a bare crystal (step 2 relates to rising). The frequency of this overtone was normalized to the fundamental resonant frequency of the quartz crystal, by dividing it by v (where v = 7).
275x397mm (300 x 300 DPI)

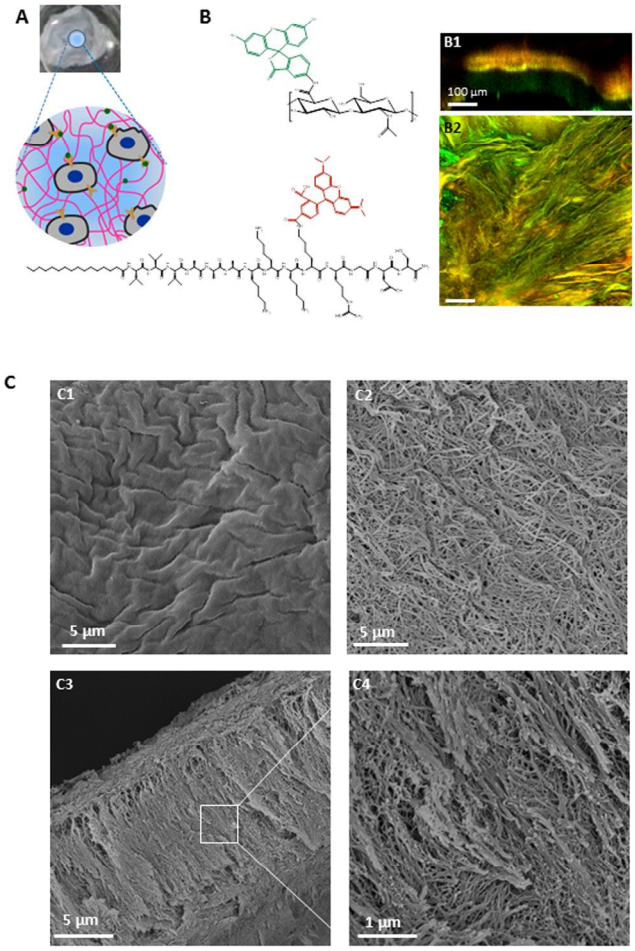

Figure 3. PA-HA membrane microstructure. A) Schematic representation of PA-HA membranes functionalized with bioactive molecules (green) interacting with cell integrins (yellow). B) Confocal microscopy images of the membranes prepared with 1% (w/v) fluorescein-HA and 2% (w/v) peptide mixture containing 0.1% K3K(Rhod)RGDS-PA. Images show the localization of HA (green) and PA (red) over the membrane surface (B2) and cross section (B1). Yellow represents the overlaping of both components. C) SEM micrographs of self-assembled membranes with 1% (w/v) HA and 2% (w/v) K3-PA, showing the surface on the polymer (C1) and peptide (C2) sides and cross section (C3, C4).
275x397mm (300 x 300 DPI)

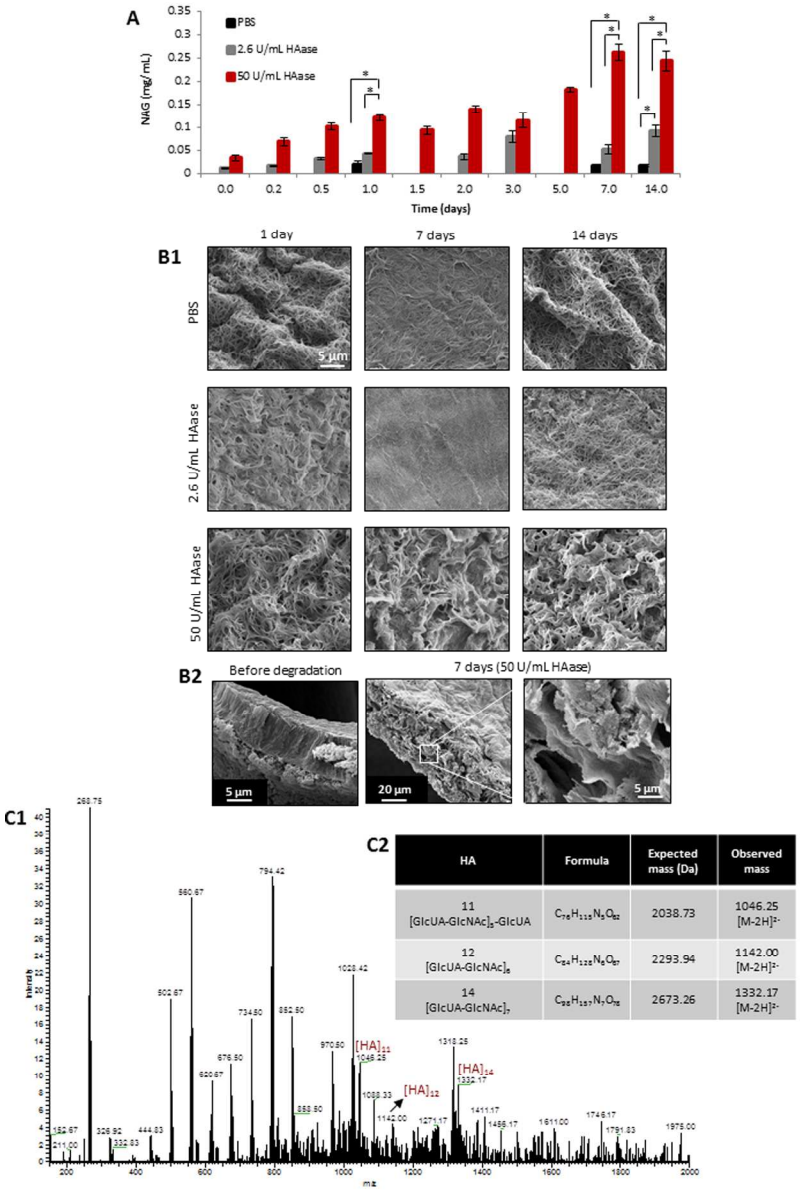

Figure 4. Degradation of PA-HA membranes. A) Quantification of N-acetylamino sugars released from K3-HA membranes in PBS and PBS containing 2.6 U/mL and 50 U/mL HAase (*p < 0.05, error bars represent standard deviation (n=3)). B1) SEM images showing differences in membrane microstructure when exposed to different hyaluronidase (HAase) concentrations up to 14 days. B2) Cross section of the membranes before and after exposure to 50 U/mL HAase evidencing that degradation is occurring not only on the surface but also inside the membrane. C1) Negative ESI-MS of the supernatant after incubating the membranes in 2.6 U/mL HAase for 7 days showing the presence of HA fragments. C2) Observed and theoretical molecular masses of HA oligosaccharides.
275x397mm (300 x 300 DPI)

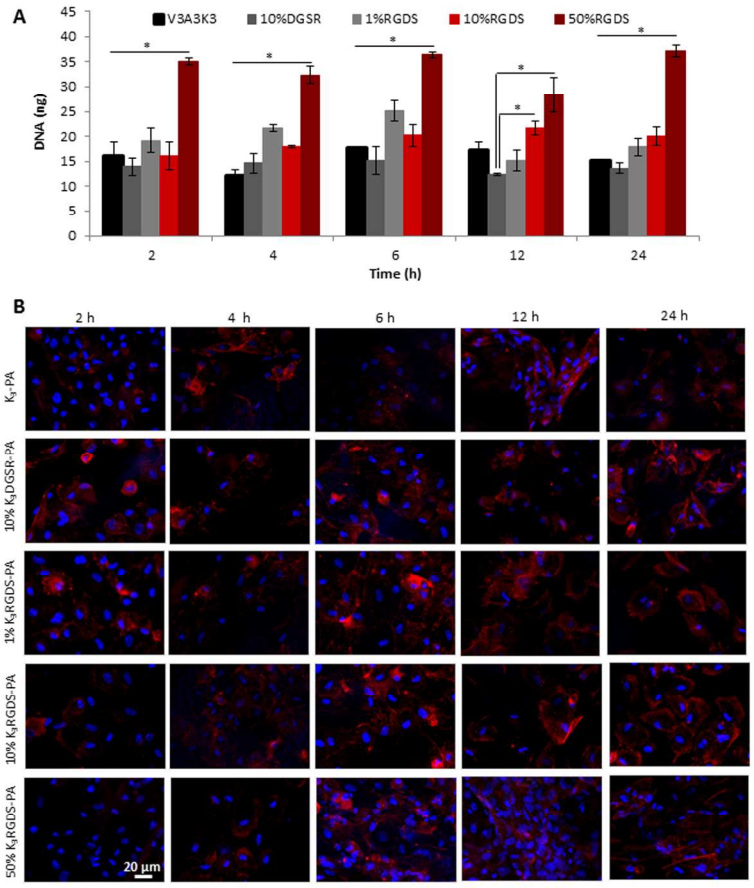

Figure 5. Cell adhesion on PA-HA membranes. dsDNA quantification (A) (*p < 0.05, error bars represent standard deviation (n=3)) and confocal fluorescence images (B) of hDFb cultured on HA-PA membranes containing 1, 10 and 50% K3RGDS-PA or 10% (w/v) K3DGSR-PA up to 24 hours of culture. F-actin was labeled with TRITC-phalloidin (red) and nuclei with DAPI (blue).
275x397mm (300 x 300 DPI)

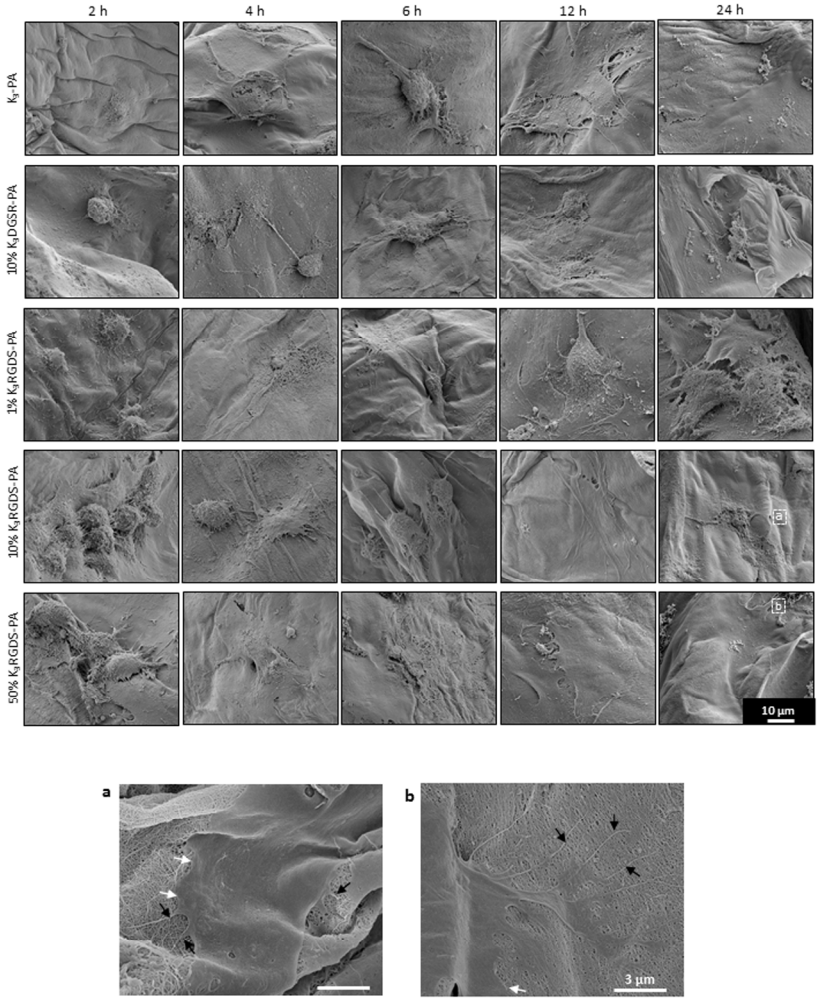

Figure 6. Cell morphology on PA-HA membranes. A) SEM micrographs of hDFb cultured on HA-PA membranes containing 1, 10 and 50% K3RGDS-PA or 10% (w/v) K3DGSR-PA. Cells were cultured on the PA side in medium without FBS up to 24 h. a) and b) show a higher magnification of the surfaces of HA-PA membranes with 10 and 50% (w/v) RGDS, respectively. Black and white arrows indicate the presence of filopodia and lamellipodia, respectively.
275x397mm (300 x 300 DPI)

Supplementary Information

Hyaluronan and self-assembling peptides as building blocks to reconstruct the extracellular environment in skin tissue

Daniela S. Ferreira[1,2], Alexandra P. Marques[1,2], Rui L. Reis[1,2], Helena S. Azevedo[1,2]

[1] 3B's Research Group - Biomaterials, Biodegradables and Biomimetics, University of Minho, Headquarters of the European Institute of Excellence on Tissue Engineering and Regenerative Medicine, AvePark, 4806-909 Taipas, Guimarães, Portugal

[2] ICVS/3B's - PT Government Associate Laboratory, Braga/Guimarães, Portugal

Peptide mass and purity

All peptides were synthesized, characterized and purified successfully. ESI and MALDI-MS were used to characterize the mass of the synthesized peptides (Fig. S1-S4, A).

The expected mass for $C_{16}V_3A_3K_3$ ($C_{58}H_{111}N_{13}O_{10}$) was 1150.58, three main peaks were found by ESI-MS, corresponding to $[M+H]^+$ m/z = 1151.30, $[M+Na]^+$ m/z= 1173.25 and $[M+2H]^{2+}$ m/z = 576.48 (Fig. S1A).
The expected mass for $C_{16}V_3A_3K_3$RGDS ($C_{73}H_{136}N_{20}O_{17}$) was 1565.98, two mains peaks were found, corresponding to $[M+2H]^{2+}$ m/z = 784.09 and $[M+3H]^{3+}$ m/z = 523.39 (Fig. S2A). For $C_{16}V_3A_3K_3$DGSR ($C_{73}H_{136}N_{20}O_{17}$) the expected mass was 1566.01, two mains peaks were found, corresponding to $[M+2H]^{2+}$ m/z = 784.03 and $[M+3H]^{3+}$ m/z = 523.41 (Fig. S3A).
The expected mass for $C_{16}V_3A_3K_3K_{rhod}$RGDS was 2108.27, two main peaks were found by MALDI-MS, m/z = 2106.54 and m/z = 1694.34, corresponding to the labeled and unlabeled peptide, respectively (Fig. S4A).

Analytical HPLC of the collected fractions showed a single peak after purification for all the PAs (Fig. S1-S4, B)

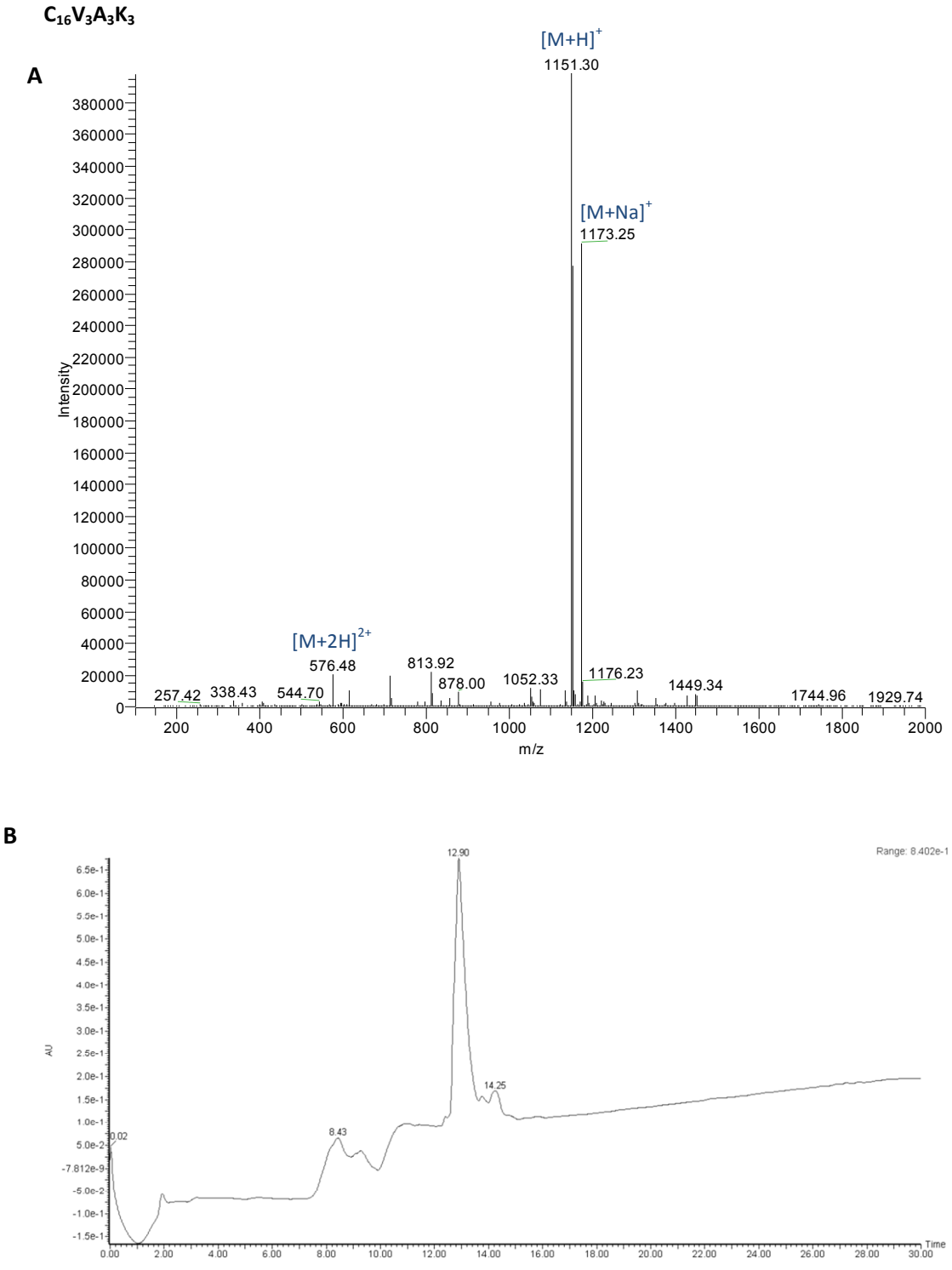

Figure S1. Representative ESI-MS data (A) and analytical HPLC trace, detected at 220 nm (B) of $C_{16}V_3A_3K_3$.

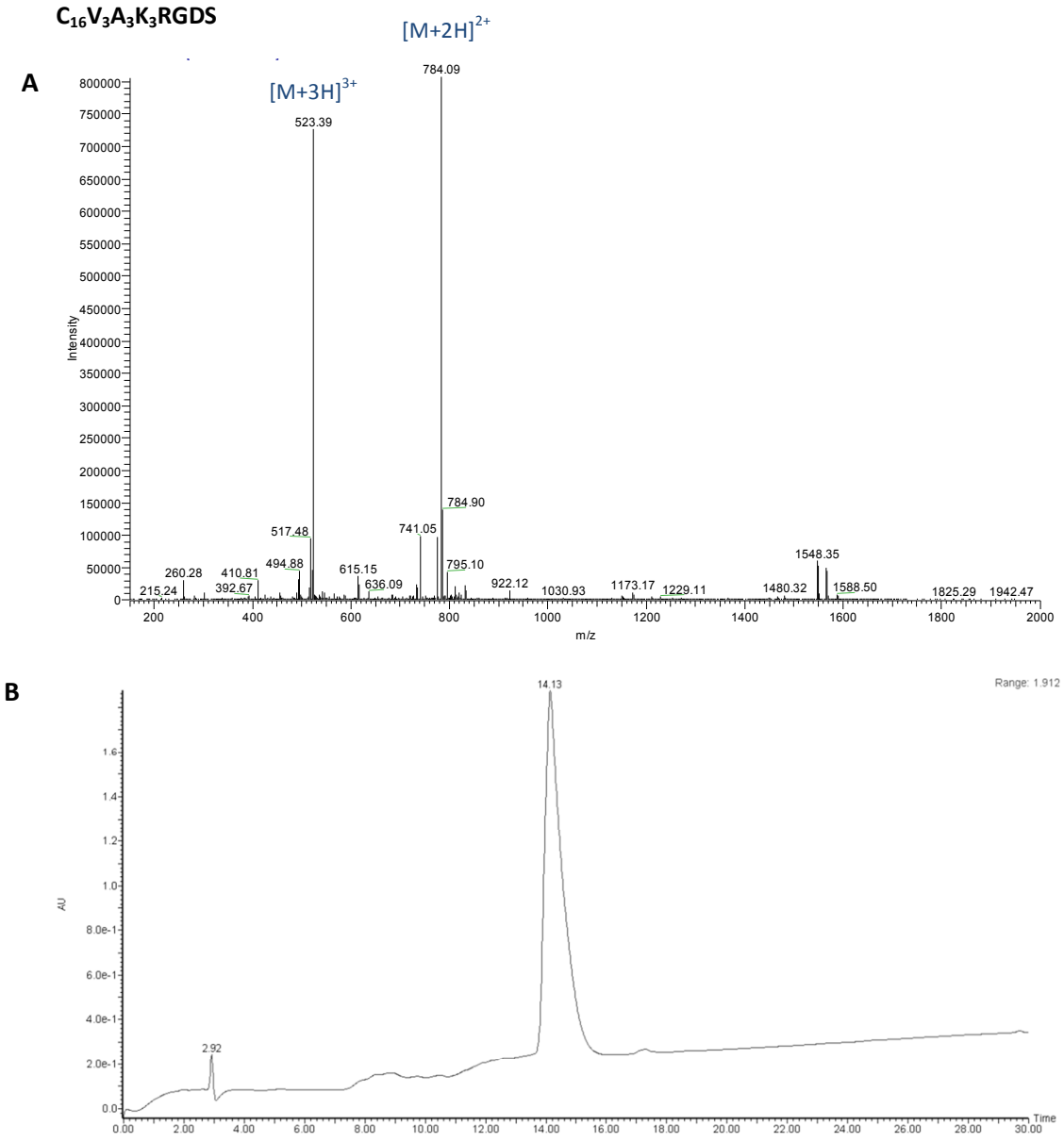

Figure S2. Representative ESI-MS data (A) and analytical HPLC trace, detected at 220 nm (B) of $C_{16}V_3A_3K_3RGDS$.

$C_{16}V_3A_3K_3DGSR$

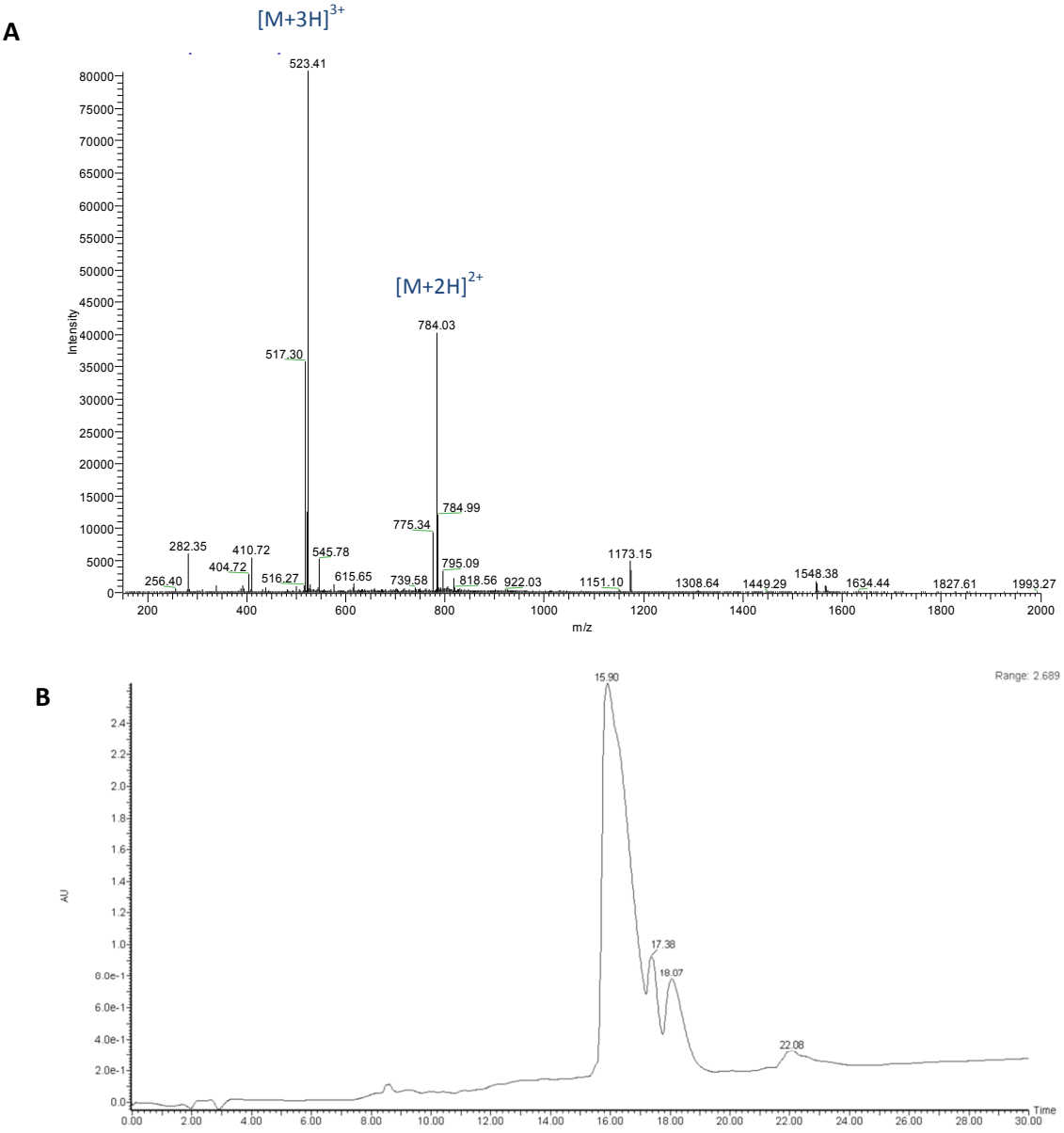

Figure S3. Representative ESI-MS data (A) and analytical HPLC trace, detected at 220 nm (B) of $C_{16}V_3A_3K_3DGSR$.

$C_{16}V_3A_3K_3K_{Rhod}$RGDS-PA

A

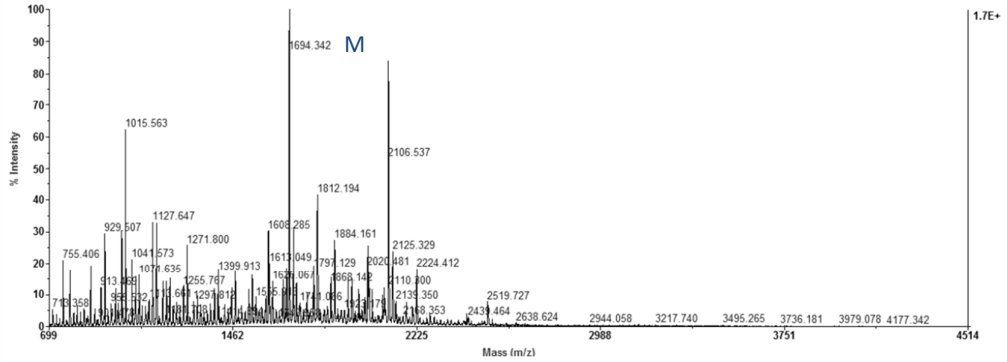

B

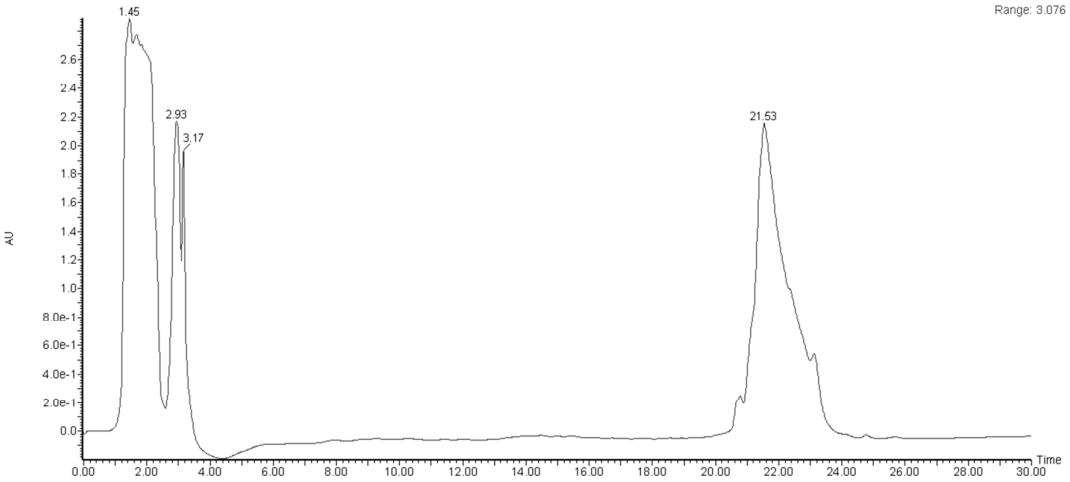

Figure S4. Representative MALDI-MS data (A) and analytical HPLC trace, detected at 220 nm (B) of $C_{16}V_3A_3K_3K_{Rhod}$RGDS-PA.

Microstructure of 50% K_3RGDS-PA membrane

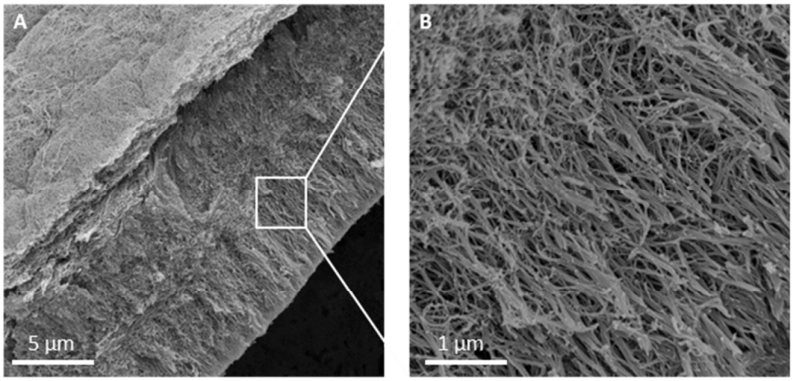

Figure S5. SEM micrographs of the cross section of a 50% K_3RGDS-HA membrane.

Identification of HA oligosaccharides from the enzymatic degradation of PA-HA membranes by mass spectrometry

ESI-MS analysis of 0.1% (w/v) HA solution (control) and of the supernatant after incubating the membranes in 50 U/mL HAase for 14 days (Fig. S6) showed the presence of HA oligosaccharides only for the samples from degradation solutions. Peaks at 331.8, 389.8 and 411.7 were detected corresponding to the masses of HA oligosaccharides with 7, 4 and 13-mers, respectively, with 4 charges m/z= 331.8 $[M_{HA7}\text{-}4H]^{4-}$; 2 charges m/z= 389.8 $[M_{HA4}\text{-}2H]^{2-}$ and with 6 charges m/z= 411.7 $[M_{HA13}\text{-}6H]^{6-}$.

The observed mass for the odd oligosaccharides are fragmentation products of ESI-MS since digestion with HAase produces even-numbered oligosaccharides. However, these fragments were not observed in the control. Therefore, the oligosaccharides found in the degradation solutions may result from the fragmentation of even oligosaccharides originated from the enzymatic digestion.

A

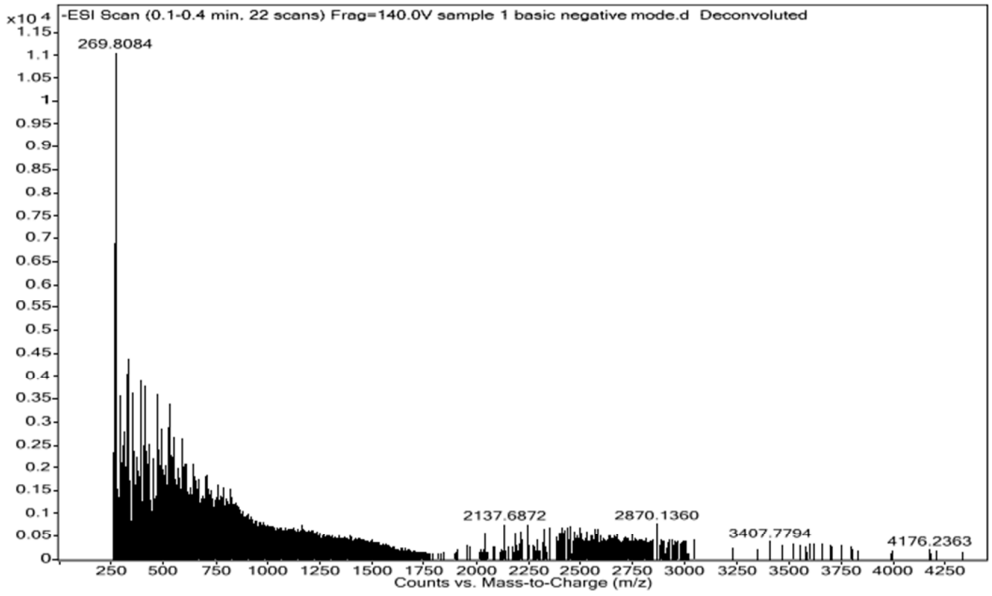

B

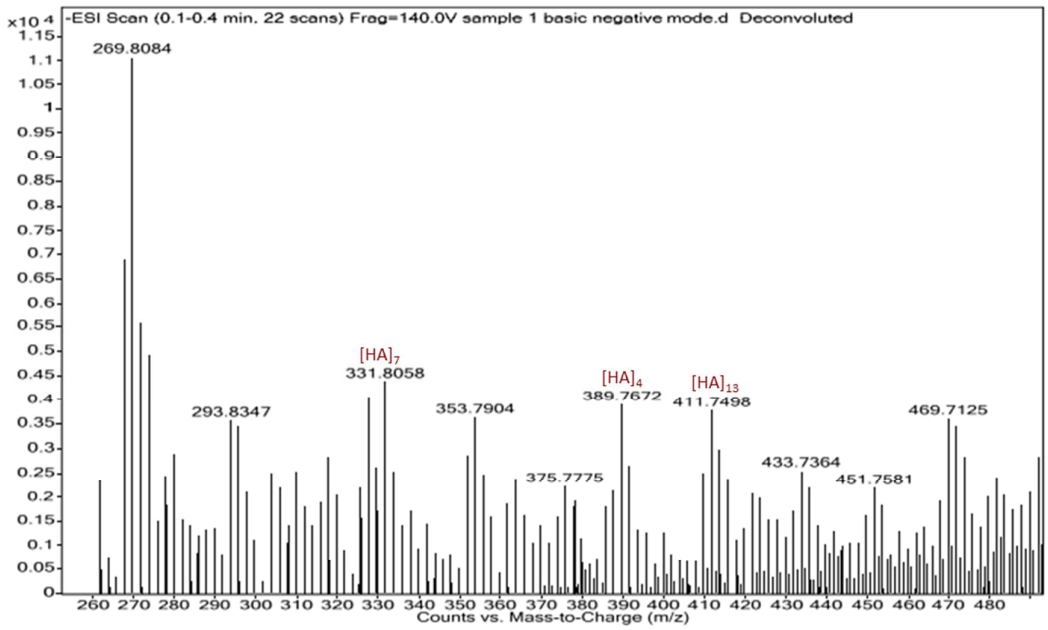

Figure S6. Negative ESI-MS of a 0.1% (w/v) hyaluronan solution (A) and of the supernatant after incubating the membranes in 50 U/mL HAase for 14 days (B).

Morphology of hDFbs cultured on PA-HA membranes in serum-containing medium

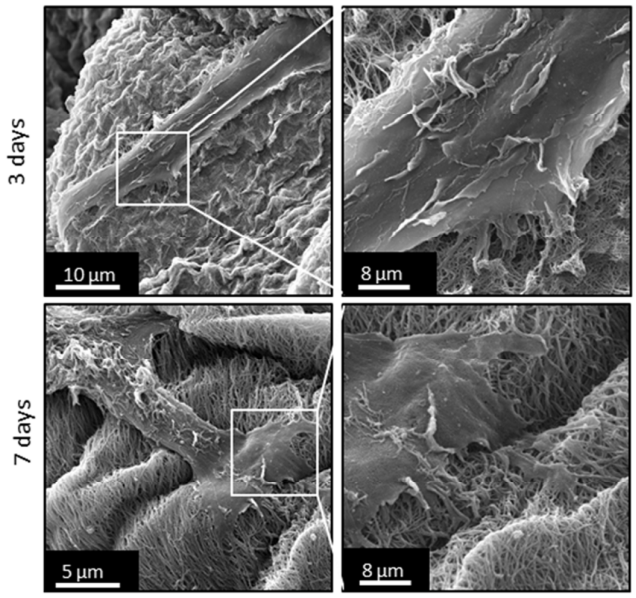

Figure S7. SEM micrographs of hDFbs cultured in K_3-HA membranes. Cells were cultured on the PA side in medium containing 10% FBS up to 7 days.

Analysis of the expression of CD44 receptor on hDFbs by flow cytomety

The expression of CD44 receptor on the surface of hDFbs was assessed by flow cytomety. Briefly, harvested cells were incubated with fluorescent monoclonal antibody against CD44, (BD Biosciences Pharmingen, USA) for 20 minutes at room temperature. Cells were then washed in aquisition buffer (0.1% sodium azide, 1% formaldehyde, in phosphate-buffered saline solution). Unlabeled controls were included to evaluate unspecific binding. Samples were analyzed using a FACScalibur(Becton-Dickinson, USA) with CellQuest analysis software (BectonDickinson, USA).

FACS analysis confirmed a high expression of CD44 (98.67%) on hDFbs. Similar values were reported in the literature for these cells[S3].

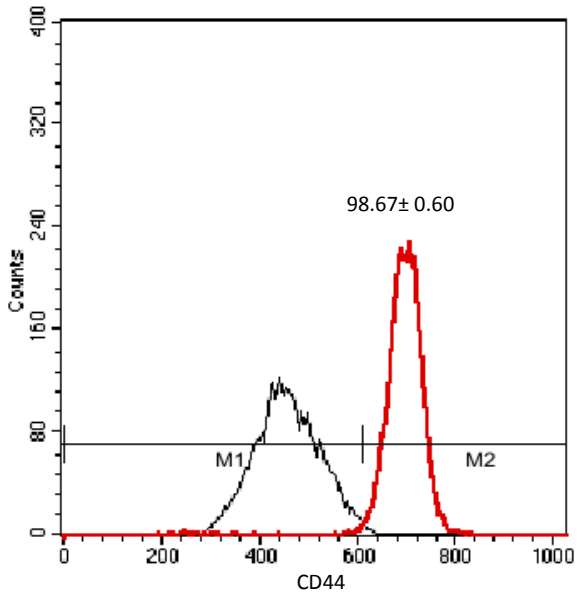

Figure S8 - Flow cytometry analysis of the expression of CD44 on the surface of hDFbs used in the cell culture studies.

hDFbs cultured on hyaluronan-based hydrogel film (non self-assembling material)

To demonstrate the role of the self-assembled component, responsible for the nanofibrillar structure of the self-assembled membranes, on the morphology of adhered cells, hDFbs were cultured on the surface of a hyaluronan hydrogel film (non self-assembling film, control). For that, Corgel® BioHydrogel, a tyramine-substituted HA hydrogel (TS-NaHy 1.5% tyramine substitution, Part #85 Corgel® Kit 1%, Lifecore Biomedical, Inc, Chaska, USA) was prepared according with the supplier's instructions and cells were cultured in serum-free conditions as described in Materials and Methods for the PA-HA membranes. The morphology of the cells was examined by SEM. Corgel® BioHydrogel is a patented hyaluronan hydrogel based on di-hydroxyphenyl linkages of tyramine substituted sodium hyaluronate (NaHy)[S1]and was shown to be biocompatible[S1-S2]. SEM images show that the HA hydrogel films presents a smooth surface (Figure S9-A) with few adherent cells with a small contact area to the surface (Figure S9-B). Furthermore, fibroblasts were completely round, without showing cell protusions (lamellipodia and filopodia) and did not flatten upon contact with the hydrogel surface.

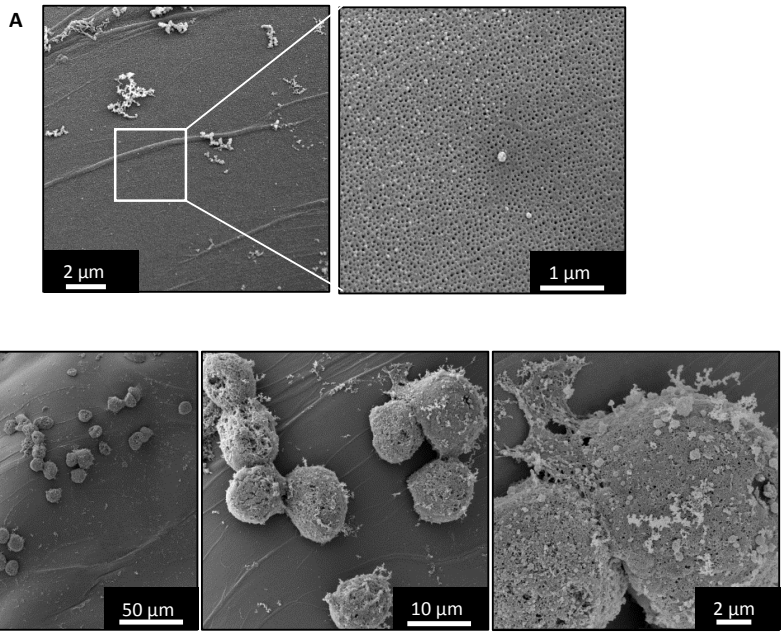

Figure S9. SEM micrographs of TS-NaHy hydrogel surface (A) and morphology of hDFbs cultured on their surface in serum-free medium for 24 h.

References

S1. A. Darr, A. Calabro, Synthesis and characterization of tyramine-based hyaluronan hydrogels. J Mater Sci: Mater Med 2009; 20: 33-44

S2. L. Chin, A. Calabro, E. E. Rodriguez, C. D. Tan, E. Walker, K. A. Derwin. Characterization of and host response to tyramine substituted-hyaluronan enriched fascia extracellular matrix. J Mater Sci: Mater Med 2011; 22:1465-1477

S3. A. Blasi, C. Martino, L. Balducci, M. Saldarelli, A. Soleti, S. Navone, L. Canzi, S. Cristini, G. Invernici, E. Parati, G. Alessandri. Dermal fibroblasts display similar phenotypic and differentiation capacity to fat-derived mesenchymal stem cells, but differ in anti-inflammatory and angiogenic potential. Vascular Cell 2011, 3:5